Epitaxy of GaAs on transferred CVD graphene

John Roberts and Tim Chen

Mentors: Xiaoqing Xu and Karl Littau

Contents

Executive summary

We attempted to implement remote epitaxy of GaAs on a GaAs substrate through transferred CVD graphene in between. We optimized and characterized a transfer method for large-area and clean graphene on GaAs substrate. We characterized a post-transfer rapid thermal annealing process and MOCVD growth. The main challenge in MOCVD growth is to suppress nanowires catalyzed by contaminants. We were able to do so in large areas of our samples and to grow a GaAs epilayer. Although our epilayer was nonuniform, we were able to mechanically exfoliate it from the GaAs/graphene substrate. Parts of the epilayer show random orientation and a rough surface, while others are preferentially (111) and smooth. This alignment does not appear to indicate remote epitaxy and the mechanism responsible for it is not known but may be alignment to the graphene layer.

Usage parameters

1. **Aixtron Black Magic** CVD graphene furnace: We used an established recipe with good results.
2. **Graphene wet transfer to GaAs using PMMA scaffold**. It is crucial to avoid wrinkles in the copper foil. We selected steps for large area and clean transfers. We investigated:
    a. **PMMA thickness**: We used 200nm and 50nm PMMA scaffolds. Thinner scaffolds may give larger graphene areas but we did not confirm this.
    b. **PMMA baking vs. drying**: We found that removing the solvents in PMMA with an overnight drying step at room temperature gave lower defect density than removing them in an oven at 80°C.
    c. **Duration of SC2 clean**: We found that longer SC2 cleaning (30 minutes) gave less metallic contamination than shorter cleaning (15 minutes) at the risk of more tears in graphene.
    d. **Number of DI water baths**: We found that more total DI water bath steps (8-10) gave significantly cleaner transfers than a minimal number of baths (4), with low risk of damage to the graphene layer.
3. **All-Win 610-r** rapid thermal annealing. We annealed graphene/GaAs samples for 30 minutes at 350°C under N_2/H_2 forming gas and observed that the surface roughness of the graphene was decreased significantly with slight doping apparent in the Raman spectrum.
4. **Aix200** MOCVD GaAs growth. Very clean graphene/GaAs samples are required to avoid nanowire growth during the nucleation step. We investigated:
    a. **Nucleation time**. We found that nucleation for 10 minutes at 450°C under 100sccm/10sccm TBAs/TMGa flow and N_2 carrier gas gave a nucleation layer around 20nm thick and that nucleation growth under the same conditions for 50-60 minutes gave a thickness closer to the 100nm target.
    b. **Nucleation temperature.** 500°C nucleation suppressed nanowires but gave irregular sites.
    c. **Nucleation V/III precursor flow ratio.** We found that higher V/III flow ratio (150sccm/10sccm instead of 100sccm/10sccm) did not suppress nanowire growth.
    d. **Substrate contamination.** We found that reducing contamination on graphene consistently gave areas of good nucleation.
    e. **Nucleation carrier gas.** We found that using H_2 carrier gas for nucleation layer growth suppressed nanowire growth.

1. Introduction

A major limitation in epitaxial growth of III-V materials for electronic and photonic applications is the cost of single-crystalline substrates. Recently, Y. Kim et al. have shown that III-V substrates including GaAs can be reused with a variant of van der Waals epitaxy known as remote epitaxy. [1] Van der Waals epitaxy involves growth on a substrate interacting with the epilayer only through van der Waals interactions, and does not require lattice matching between the grown material and the substrate. [2] Graphene provides an ideal surface for this type of growth, and in the past decade van der Waals epitaxy has been demonstrated on graphene. [3] Y. Kim et al show that, when epitaxial growth proceeds on a graphene layer transferred to a substrate of the same material as the epilayer, the epilayer can register to the substrate because the graphene monolayer does not completely screen the potential of the underlying lattice. They demonstrate the use of this technique to grow single-crystalline epilayers of III-V materials epitaxially registered to the substrate. The weak van der Waals interaction with the graphene still allows easy release of the epilayer using mechanical exfoliation. Once the epilayer is transferred to another substrate for use in a device, the original graphene-coated substrate may be reused. Kim et al show that this growth process yields GaAs films with the same quality as homoepitaxial growth.

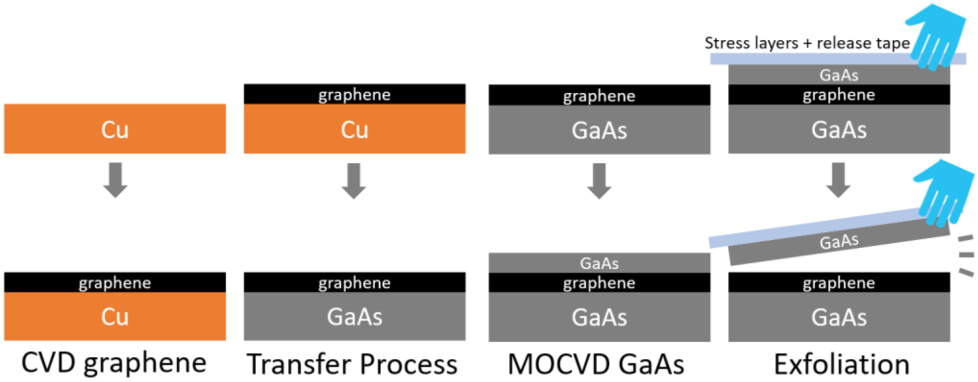

We attempted to implement this process in the ExFab using the Aixtron Black Magic Pro graphene furnace and the Aixtron 200 MOCVD furnace. The process has four major steps: graphene synthesis by CVD, graphene transfer, GaAs epitaxy by MOCVD, and exfoliation. In this report, we document the details of each step and our characterization of the process.

---

[1] Y. Kim *et al*., 'Remote epitaxy through graphene enables two-dimensional material-based layer transfer', Nature **544**, 340–343 (2017)

[2] A. Koma *et al*., 'Fabrication and characterization of heterostructures with subnanometer thickness', Microelectronic Eng. **2** (1-3), 129 (1984).

[3] K. Chung, C.-H. Lee, and G.-C. Yi, 'Transferable GaN Layers Grown on ZnO-Coated Graphene Layers for Optoelectronic Devices', Science **330** (6004), 655-657 (2010)

2. CVD graphene synthesis

Chemical vapor deposition is widely used for graphene production. Compared to other methods, it produces large area and decent quality graphene. One of the most common CVD processes uses CH_4 and H_2 as reactants and copper substrate as a metal catalyst under low pressure. Because of the self-limiting growth on the copper surface, it has relatively simple process flow.

2.1. Copper foil

Our growth substrate is 99.9% purity copper foil, 18µm thick, from JX Nippon Mining & Metals. JX Nippon Mining & Metals is a Japanese company, so the international lead time is long and can easily be weeks or months. For CVD graphene, they offer us two thickness options: 18um and 35um. The more easily accessible copper foil is the 99.8% foil from Alfa Aesar company. It is the bare copper foil and can be found widely in graphene literature. Alfa Aesar also have high purity options (99.9%, 99.99% etc.). However, those higher purity foils are coated by chemicals as protection layers. To use them in graphene CVD process, additional pretreatments are needed to remove the coatings. [4]

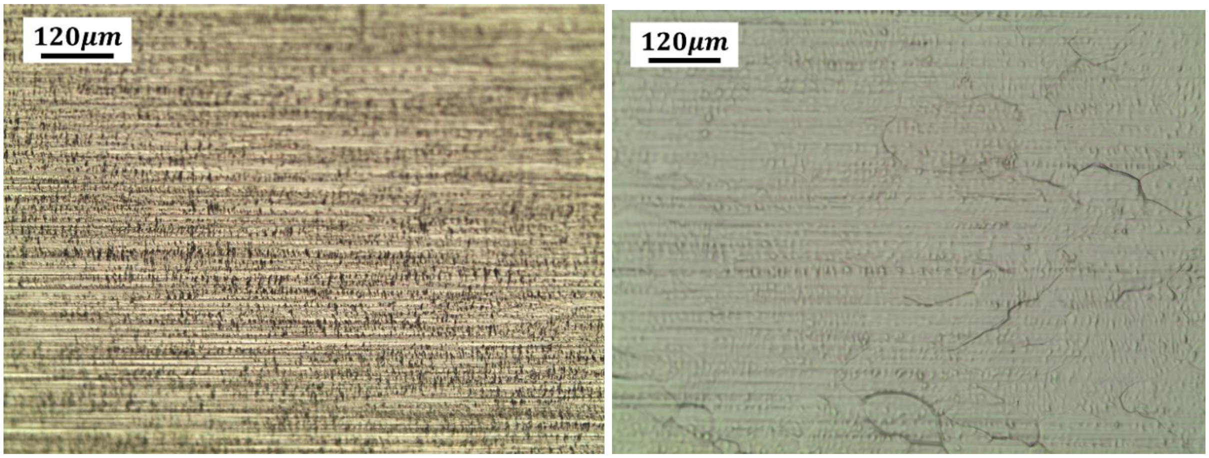

Figure 1. OM images of 99.9% bare copper foil from JX Mining (left) and graphene/copper after CVD process (right).

2.2. Pretreatment of Copper Foil

We cut the foil into roughly 4 by 4 inches square. Smaller pieces are not recommended because they might fall off the CVD susceptor while pumping/venting. To remove surface oxide and any possible morphology related effects, we introduce acetic acid in the pretreatment of copper foil [4] [5]. We soaked the copper foil in acetic acid for 1 hour. After the acetic acid, the copper foil is briefly soaked in DI water bath, and then rinsed by DI water. When the copper foil is dry, it is ready for the CVD process.

---

[4] N.C. Wang and C.M. Neumann, 'Black Magic Pro 4" Graphene Furnace Development and Characterization', Stanford University EE412 final report (2015): https://snf.stanford.edu/SNF/equipment/chemical-vapor-deposition/low-pressure-cvd/CVD-graphene

[5] K. L. Chavez et al., A Novel Method of Etching Copper Oxide Using Acetic Acid, Journal of The Electrochemical Society, 148 -11 G640-G643 (2001)

2.3. CVD Process

Aixtron Black Magic Pro is a specialized reactor for CVD graphene growth in SNF. It has a vertical showerhead design, with top and bottom graphite heaters to ensure that the temperature and growth is uniform across the substrate. We used the recipe CUFOIL_REV2, with process gases CH_4, H_2, Ar at 10mbar and 1050˚C

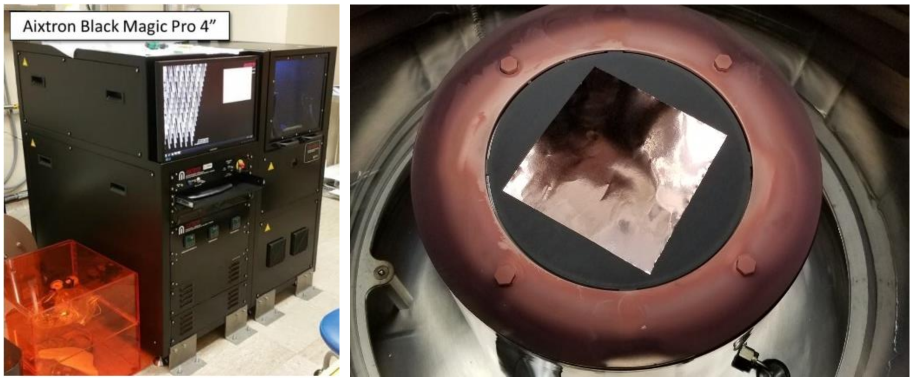

Figure 2. Aixtron Black Magic Pro CVD chamber (Left) outside and (Right) inside.

We used the standard recipe developed by the superusers of this tool, [6] with good results. Raman spectroscopy is commonly used to characterize the quality of graphene. Excitations in the Raman spectrum reveal the number of layers, defects, strains and doping. We took Raman spectrum directly on graphene-grown copper foil. Due to the fluorescence effect, there is strong background in spectrum, but the graphene peaks can still be seen clearly (Figure 3 blue line). The position of the peaks agrees well with known values. After background subtraction (Figure 3 red line), the ratio of the integrated peak intensity of 2D and G band is 2.28, which is larger than 2.0 that indicates monolayer graphene. The intensity of D band is low, which means that the defect is small, and that the quality of the graphene is good.

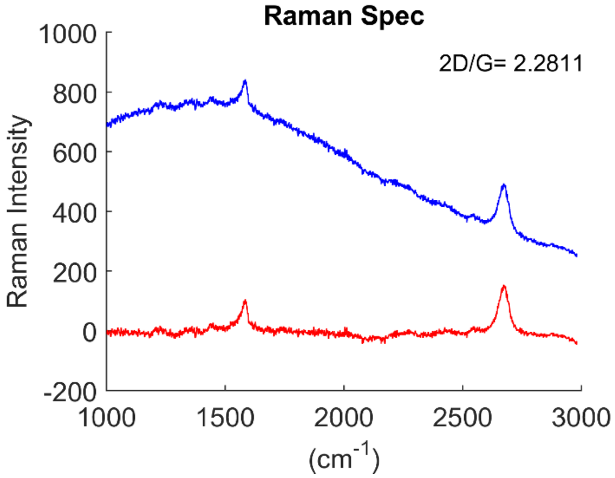

(cm^{-1})	**G**	**2D**	**D**
Paper[7]	1580	2690	1350
Measured	1585	2673	1360

Figure 3. Raman spectrum of graphene on Cu. (Blue) Raw data. (Red) After background subtraction.

---

[6] N.C. Wang and C.M. Neumann, ‘Black Magic Pro 4” Graphene Furnace Development and Characterization’, Stanford University EE412 final report (2015)

[7] Ferrari, A. C. Solid State Commun. 2007, 143, 47-57 (2007)

3. Optimized transfer of CVD graphene to GaAs substrates

We transferred CVD graphene grown on copper foil to GaAs substrates using a standard PMMA-assisted wet transfer technique. Although cleaner wet transfer methods using other polymers exist [8][9], we used a PMMA-based wet transfer because it has previously been characterized using equipment at Stanford [10] and because it was successfully used for remote epitaxy by Y. Kim *et al*.

In this wet transfer technique (figure 4), PMMA is spun on copper foil after graphene growth. The foil/graphene/PMMA is floated on copper etchant, removing the foil. A glass slide is used to scoop out the graphene/PMMA, which is transferred to a series of cleaning baths based on a modified RCA cleaning procedure. The substrate is used to scoop the graphene/PMMA out of the final bath. The substrate/graphene/PMMA stack is baked and then the PMMA is removed by soaking in acetone.

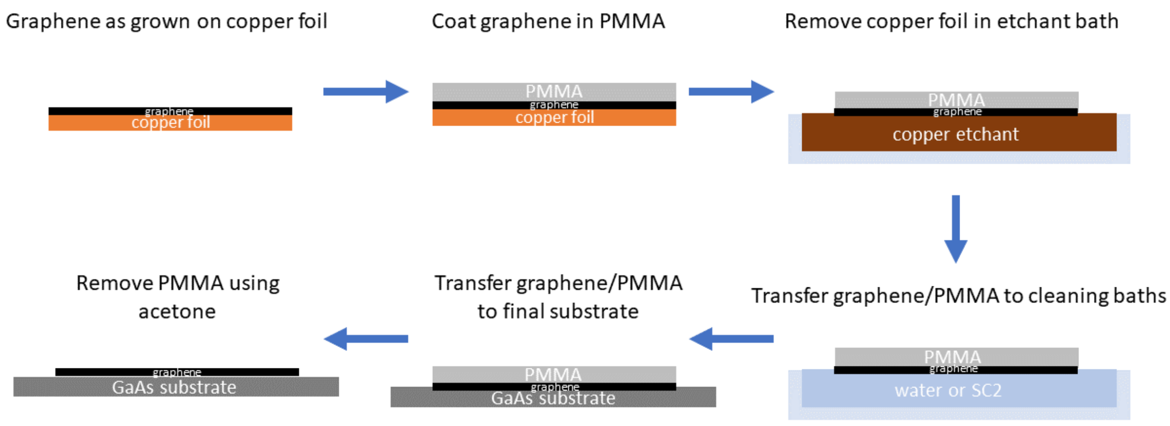

Figure 4. Major steps of the graphene transfer process using a PMMA scaffold.

The starting point for the development of our procedure was the previous EE412 report [10] characterizing the Aixtron Black Magic BM Pro graphene furnace at Stanford. We also referred to methods in the literature on high-quality, large-area graphene transfer [11] [12]. Based on our survey of the literature two parameters appeared significant:

1. Thickness of the PMMA scaffold. Some references recommend use of a thinner scaffold in order to promote flexibility of the graphene layer during transfer [13], which may reduce tears.

---

[8] T. Hallam *et al*., 'Strain, Bubbles, Dirt, and Folds: A Study of Graphene Polymer-Assisted Transfer', Adv. Mat. Interfaces **1** (6), 1400115 (2014). DOI: 10.1002/admi.201400115

[9] J.D. Wood *et al*., 'Annealing free, clean graphene transfer using alternative polymer scaffolds', Nanotechnology **26** (5), 055302 (2015).

[10] N.C. Wang and C.M. Neumann, 'Black Magic Pro 4" Graphene Furnace Development and Characterization', Stanford University EE412 final report (2015)

[11] M.H.D. Guimarães *et al*., 'Atomically Thin Ohmic Edge Contacts Between Two-Dimensional Materials', ACS Nano **10** (6), 6392 (2016). DOI: 10.1021/acsnano.6b02879

[12] Y. Han *et al*., 'Atomically Thin Graphene Windows That Enable High Contrast Electron Microscopy without a Speciment Vacuum Chamber', Nano Lett. **16** (12), 7427 (2016). DOI: 10.1021/acs.nanolett.6b03016

[13] C.S. Ruiz-Vargas, Ph.D. thesis, Cornell University, 2013. Retrieved from https://park-lab.uchicago.edu/sites/park-lab.uchicago.edu/files/uploads/Publications/Theses/CarlosRuiz-Vargas_0.pdf

2. Method by which the solvent is removed from PMMA. Baking after spinning PMMA is common, but some references recommend drying the PMMA at room temperature instead. [14] It is unclear what the advantage of removing the baking step is. This more gradual process may strain the graphene less, at the risk of incomplete removal of the solvent.

Ideally, the transferred graphene films would be monolayer, have low defect density, cover a large area continuously, and have minimal residue from copper, etchant and PMMA. We checked that our graphene was monolayer with acceptable defect density using Raman spectroscopy, and characterized coverage and residue using optical microscopy and SEM. We initially optimized our transfers for coverage since we expected that this would be a limiting factor in the achievable area of remote epitaxy. After it became clear that residue caused MOCVD nanowire growth, a more serious problem, we shifted our focus from coverage to cleanliness. To some extent there are tradeoffs between these qualities. Longer SC2 clean times and more consecutive DI water baths can reduce residues at the risk of more damage to the graphene. Four of our rounds of transfer were affected by a bad batch of copper etchant that caused extra residues. A summary of all the transfers we performed is given in table 1.

Table 1. Summary of all graphene transfers

Samples transferred (number)	Parameters varied	Major changes to procedure	Notes and outcome
G1B (1)	None	Initial attempt to transfer	Sample appeared monolayer but with many tears and residues
G1D (1)	None	Add backside O_2 plasma etch	Sample still had many tears and residues
G2A-D, G3A-D (8)	PMMA thickness, baking	Added PET for PMMA spinning. Removed SC1 clean. Added overnight drying step and N_2 blow dry	First attempt to vary PMMA parameters. However unbaked sample coverage and residue much better than baked because of other factors (scotch vs. Kapton tape, tape removal method, hotplate baking, blunt scissors). Unbaked samples had high graphene defectivity.
G4A-H (8)	PMMA thickness, baking	Baked in oven instead of hotplate. Longer PMMA drying time for unbaked PMMA. Consistent use of scotch tape, sharp scissors. New batch of etchant.	Comparable coverage for baked and unbaked samples (baked samples significantly better than last G3A-D). Unbaked samples had much lower defectivity. However new batch of etchant caused significant residues.
G4I-L (4)	PMMA thickness	All samples baked. Less concentrated HCl (10%, was 37%) for GaAs oxide strip.	Still affected by residues. Otherwise close to final transfer procedure.
G6A-F (6)	Copper etchant times	Longer copper etchant times (2, 4, 12 hours) in attempt to remove residue	None of the samples had significantly improved residue.
G6H-M (6)	Copper etchant batch (old vs. new), copper etch times	More attention to rinsing after acetone	Samples with new batch of etchant (G6L, G6M) had residue while samples with old etchant (G6G-K) were much clearer. Conclude that new etchant batch causes residues.
G6N-U (8)	Number of DI water baths, SC2 time	For some samples increase number of DI baths to 8 from 4. Try longer (30 min.) SC2 clean. No overnight DI bath (time constraints). Use less	Shifted focus to removing what was left of metallic residue. Samples with more DI baths were much cleaner. Effect of longer SC2 clean ambiguous

---

[14] A.M. van der Zande *et al.*, 'Large-Scale Arrays of Single-Layer Graphene Resonators', Nano Lett. **10** (12), 4869 (2010). DOI: 10.1021/nl102713c

		concentrated HCl (3%) for GaAs oxide strip.	(possibly cleaner but more tears). Less concentrated HCl
G6V-Z,α-δ (9)	SC2 time	Increase number of DI baths to 10.	All samples affected by violent SC2. Longer SC2 times appear cleaner.

Our optimized transfer procedure is given below and depicted in figure 5-7. The steps altered for very clean transfers are marked in bold (number of DI water baths and SC2 clean time).

3.1. Optimized graphene transfer procedure[15]

1. **Attach copper foils to PET supports.** Cut copper foil into roughly 1-2cm squares. Cut PET into larger squares and bake at 80°C in an oven until they are flat. Rinse PET squares with IPA and blow dry. Flatten copper foil squares between two glass slides using weighing paper (available at the bio store) to avoid direct contact with glass. Press down quickly but firmly. Place PET squares on individual pieces of weighing paper, then tape copper foil squares onto PET squares using green Scotch tape. Cut the squares so that the weighing paper is removed from the bottom, leaving only copper foil squares taped on PET squares. It is crucial throughout these steps to avoid wrinkles in the copper foil.
2. **Spin PMMA.** For thick PMMA we used PMMA 950 A4, 3000 RPM (around 200nm) and for thin PMMA we used PMMA 950 A2, 3000 RPM (less than 50nm). One indicator that the foil is sufficiently flat is the appearance of a ‘frame’ inside the foil area where the PMMA thickness builds up near the tape.

   Note: We suspect that thin PMMA leads to better coverage but have not been able to verify this. This would be easy to investigate on a silicon/SiO_2 substrate with 90nm or 280nm oxide for graphene visibility but is difficult to evaluate on GaAs with no oxide.

3. **Remove PMMA solvent**. Either:
   a. Bake foil (still taped to the PET support) in an oven (not a hotplate) at 80°C for 10 minutes, ***or***
   b. Let the solvent evaporate overnight. This may lead to graphene with lower defect density
4. **Remove PET support**. Holding one corner of the PET support with tweezers, cut perpendicular to the tweezers across the far edge of the copper foil and toward the tweezers so that the part of the copper foil held by tape is cut off. Rotate the foil 180° and repeat this procedure, then cut off the remaining two edges of the foil. Remove the PET from the back of the copper foil.

   Note: Avoid cutting at a right angle into a dangling edge since this can cause the foil to wrinkle.

5. **Etch copper foil away.** Float the copper foil/graphene/PMMA on ferric chloride copper etchant (Transene CE-100) in a plastic beaker, graphene/PMMA-side up. Etch for about one hour. We performed this step and subsequent steps at wbflexcorr-1 and -2 in SNF.

   Notes: Avoid glass/quartz beakers for all of the following steps since the graphene/PMMA will tend to stick to the edges more than in Teflon beakers. Although

---

[15] Many of the details are thanks to advice from Michelle Chen and Ning Wang.

the copper will visibly disappear within about 15 minutes, the longer etch ensures that there is no remnant copper. For this and subsequent steps we tried to use small beakers, typically 100mL or 150mL, since this minimizes use of chemicals while allowing for parameter variation between samples in several different beakers.

6. **Transfer to DI water baths**. Using a piranha-cleaned glass slide, scoop the graphene/PMMA out of the copper etchant and transfer it to a DI water bath. Use at least two consecutive DI water baths, 10 minutes each. **For low-residue transfers**, use 4-5 DI water baths at this step.

   Note: There appears to be little disadvantage to adding more baths since the risk of destroying the sample during one of these transfers is low. The SC2 clean tends to be riskier. For most of our transfers we used 2 baths at this step (4 total), but for the very clean transfers we used 4-5 baths at this step (8-10 total). The final bath in this step can be overnight, but this is not necessary – because of time constraints our clean transfers did not have an overnight step.

7. **SC2 clean**. Mix SC2 (6:1:1 DI water:37% hydrochloric acid:30% hydrogen peroxide) in a plastic beaker. This step is intended to remove metal contamination as part of a modified RCA transfer. Transfer the graphene/PMMA to SC2 using a glass slide. Let the graphene/PMMA float on SC2 for at least 10 minutes. **For low-residue transfers**, longer SC2 cleans appear to give less metal residue (we used 30 minutes SC2 for our clean transfers).

   Note: bubbles from the SC2 can damage samples. Avoid sudden movements of the beaker. Avoid using unopened bottles of H_2O_2 since they can cause more bubbles.

8. **Transfer to DI water baths.** Repeat step 6. Use at least two consecutive water baths, and **for low-residue transfers** use 4-5 water baths.
9. **Scoop the graphene/PMMA onto final substrate and dry**. We removed the oxide on our GaAs {001} substrate by submerging in 3% HCl for 30 seconds, followed by rinsing in water. This must be done immediately before the graphene scoop so that the oxide does not grow back. As soon as the graphene/PMMA is scooped onto the substrate from the final water bath, blow with a nitrogen gun at close range starting from the center of the graphene/PMMA and spiraling outwards.

   Notes: Using more concentrated HCl can cause damage to the substrate. After this step it is crucial for MOCVD growth to avoid contamination to the sample. Normally the HCl treatment would be done immediately before the growth. Since there is necessarily a long time in our process between the HCl treatment and the MOCVD growth, after the treatment the sample should not be touched with gloves (only tweezers). Avoid breathing on the sample by using a mask whenever handling it.

10. **Dry overnight at room temperature**
11. **Bake sample and remove PMMA using acetone.** We baked at 50°C for 30 minutes, then submerged the samples in acetone for 30 minutes to dissolve the PMMA. Rinse with acetone and IPA and blow dry with a nitrogen gun. This bake removes any remaining water from between the graphene and substrate. We performed these steps at wbexfab_solv near Headway3.

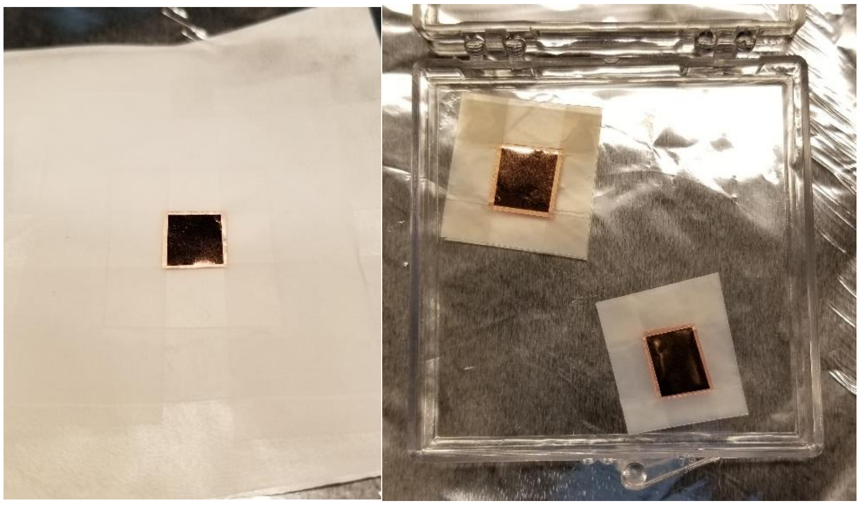

Figure 5. Copper foil with grown graphene taped to PET on weighing paper (left), and after weighing paper is cut off but the bottom part is removed (right)

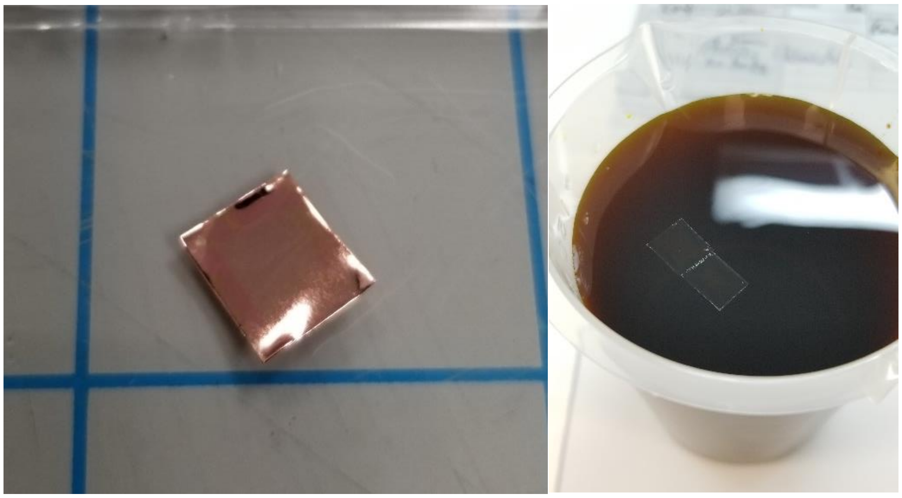

Figure 6. Copper foil/graphene with PMMA (left) showing the 'frame' pattern, and graphene/PMMA floating on copper etchant (right) in 150mL beaker.

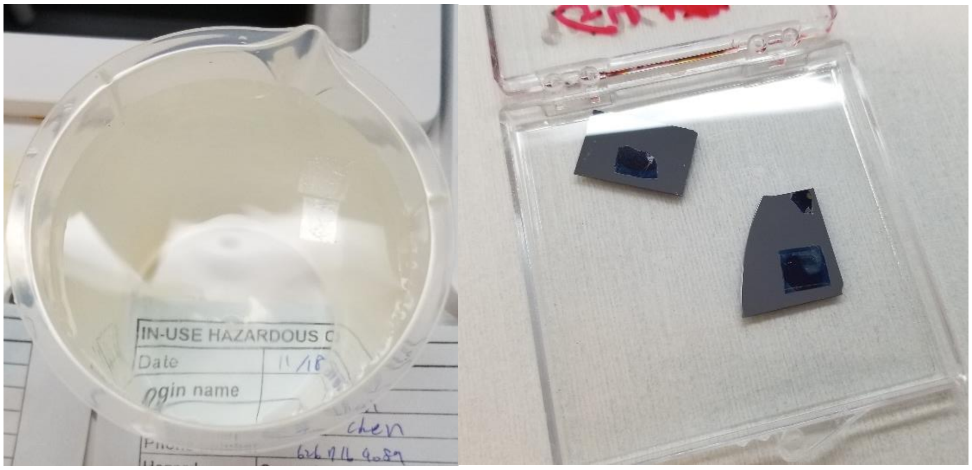

Figure 7. Graphene/PMMA floating on water (left) and after transfer to GaAs (right) before PMMA is dissolved.

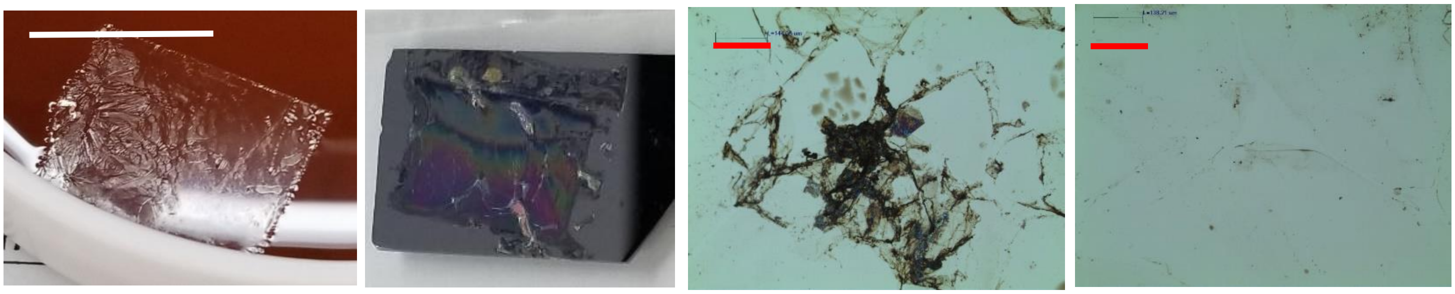

Figure 8. An initial attempt at graphene transfer: graphene/PMMA floating on copper etchant (scale bar approx. 1cm); graphene/PMMA on the final GaAs substrate; optical microscope image of the worst area in the graphene; OM image of the best area of graphene (OM scale bars 150µm). Sample G1D

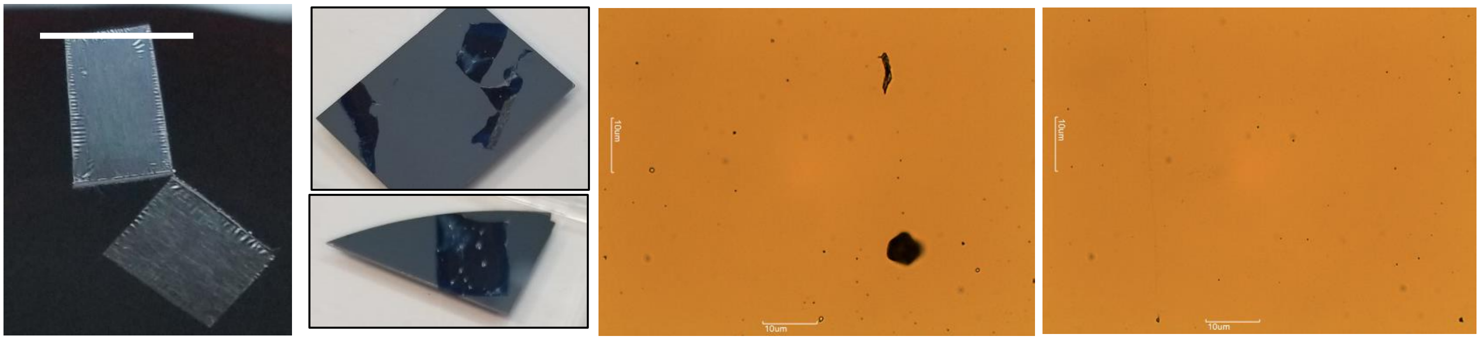

Figure 9. Graphene transfer optimized for large-area coverage. Graphene/PMMA floating on copper etchant (scale bar approx. 1cm); graphene/PMMA on the final GaAs substrate; OM image of the worst part of the graphene; OM image of the best part of the graphene (OM scale bars 10µm). Sample G2C.

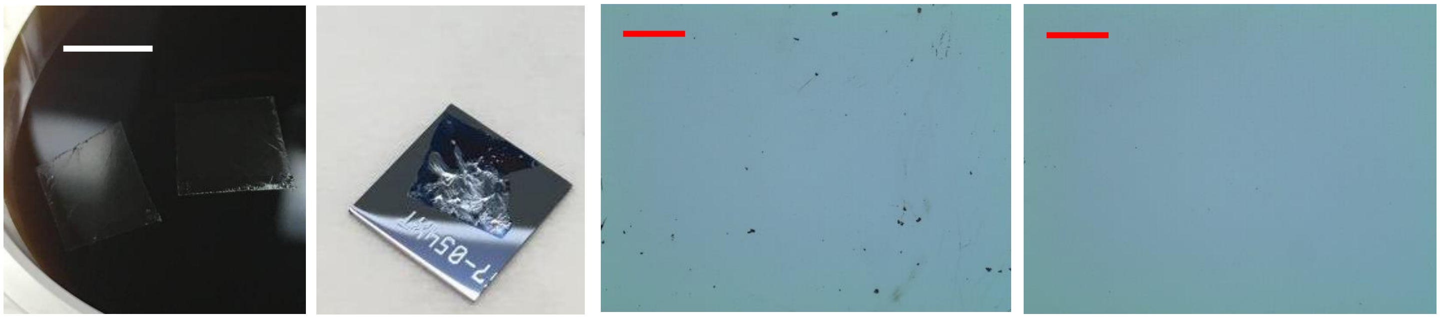

Figure 10. Graphene transfer optimized for cleanliness. Graphene/PMMA floating on copper etchant (scale bar approx. 1cm); graphene/PMMA on the final GaAs substrate (after damage from violent SC2 caused by a freshly opened bottle of H_2O_2); OM image of the worst part of the graphene; OM image of the best part of the graphene (OM scale bars 150µm). Sample G6V

4. Characterization of graphene transfer

We characterized our transferred graphene using Raman spectroscopy and optical microscopy as well as SEM. In this section we will also discuss our conclusions about the effects of PMMA thickness and baking.

4.1. Raman spectroscopy

We used Raman spectroscopy to check that the graphene was monolayer and had acceptable defectivity. The three relevant peaks in the Raman spectrum of graphene [16][17] are the D peak around 1350cm^{-1}, the G peak near 1590 cm^{-1}, and the 2D peak near 2700 cm^{-1}. The D peak is due to scattering from a Brillouin zone-corner phonon corresponding to a breathing mode of a single atomic ring. As a result it is forbidden by symmetry and requires a point defect to be active, and so the D peak intensity can be used as a measure of defect density in graphene. The 2D peak is an overtone of the D peak but is not forbidden by symmetry because two phonons are involved. The G peak corresponds to scattering from a single phonon at the zone center.

The signatures of monolayer graphene are a G peak smaller than the 2D peak, as well as a narrow 2D peak. We adopted the rule of thumb that the integrated Lorentzian weight of the G peak should be less than half the 2D peak ($I_G < I_{2D}/2$) which has been used by researchers at Stanford [18]. Additionally, the integrated D peak should be around 10% of the G peak for acceptable defect density.

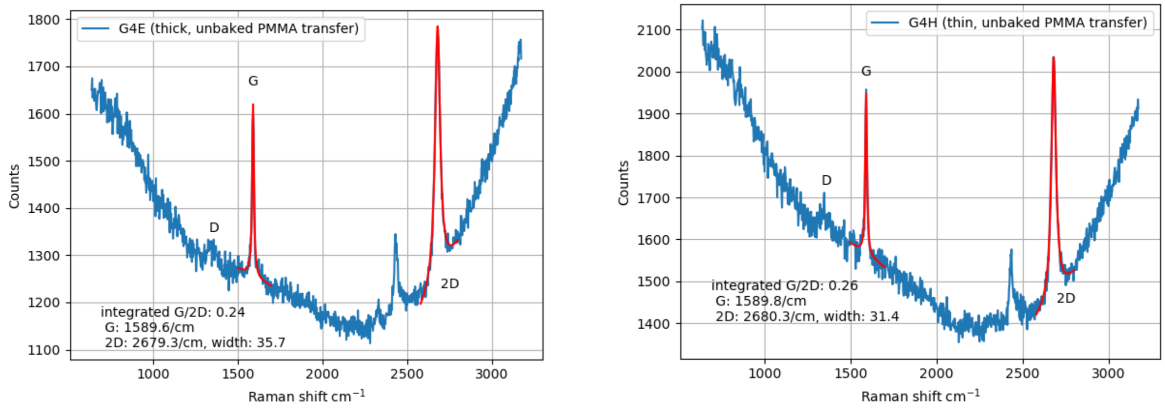

Figure 11. Raman spectra of graphene transferred using thick (left) and thin (right) unbaked PMMA. Thick PMMA is around 200nm (PMMA 950 A4, 3000 RPM) and thin PMMA is less than 50nm (PMMA 950 A2, 3000 RPM)

---

[16] A.C Ferrari *et al.*, 'Raman Spectrum of Graphene and Graphene Layers', Phys. Rev. Lett. **97**, 187401 (2006)

[17] A.C. Ferrari and D.M. Basko, 'Raman spectroscopy as a versatile tool for studying the properties of graphene', Nat. Nanotech. **8**, 235 (2013) DOI: 10.1038/NNANO.2013.46

[18] Conversation with Ning Wang

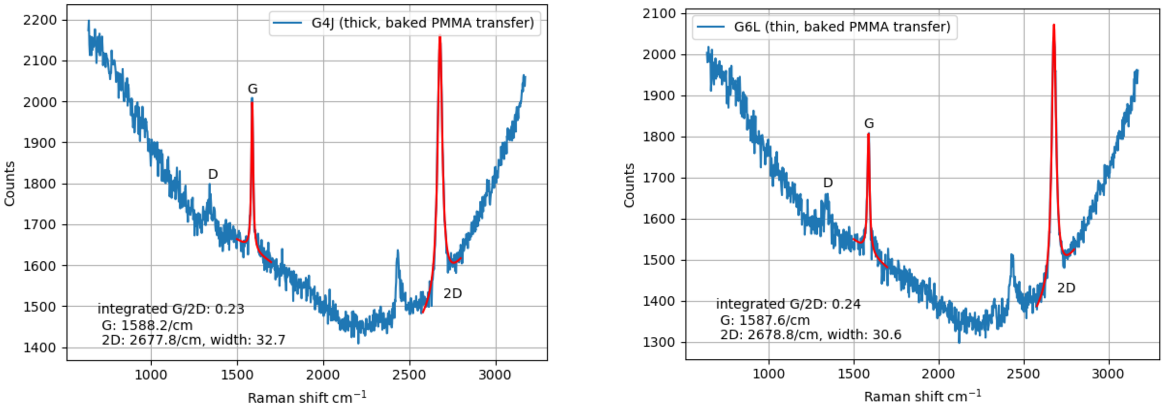

Figure 12. Raman spectra of graphene transferred using thick (left) and thin (right) baked PMMA. The defect peak appears larger than for unbaked PMMA (figure 11). Thick PMMA is around 200nm (PMMA 950 A4, 3000 RPM) and thin PMMA is less than 50nm (PMMA 950 A2, 3000 RPM)

We performed measurements using the Horiba LabRAM and XploRA Raman spectrometers in SNSF. Raman measurement of graphene on GaAs poses a unique challenge because the excitation energy is above the direct bandgap of the substrate. As a result there is little reflection and the Raman signal is weak. Additionally, we found that the LabRAM CCD is damaged (likely by direct illumination from the elastic peak when the spectrometer was moved to dangerously low wavenumbers) in such a way that for small signals the lower-wavenumber part of the window receives less signal than the higher-energy part. This hindered our efforts to use Raman spectroscopy until we switched to the XploRA spectrometer. All spectra taken using the XploRA give a peak around 2450cm^{-1} that appears even without a sample (spectrum of a new glass slide) and is probably not related to our samples.

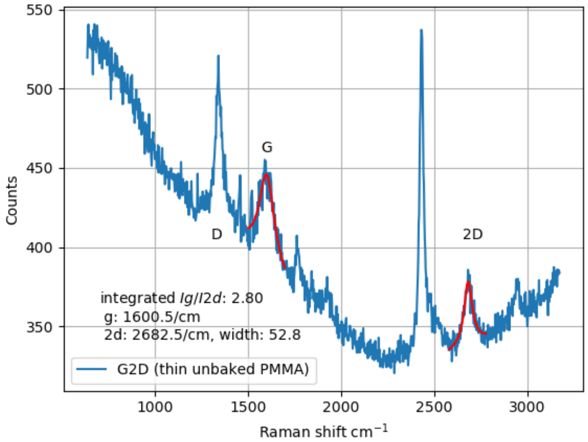

Figure 13. Raman spectrum of sample G2D showing high defect density caused by not baking the PMMA and not allowing sufficient time for the solvent to evaporate (drying time about 20 minutes).

We found that all of our final transfer techniques give monolayer graphene with acceptable defect density (figures 11-12), but still higher than what is possible with the Aixtron graphene furnace [3]. It appears that baked PMMA gives slightly more defective graphene than unbaked PMMA. However, quantifying the defect density was difficult because of the noisy, low-intensity signal. The only case in which we found that the graphene was very highly defected was for transfers using unbaked PMMA with short PMMA drying times (around 20 minutes) instead of several hours or overnight (figure 13)

4.2. Coverage and tears: optical microscopy and SEM

We initially aimed to maximize the area of continuous graphene coverage of our samples. The coverage is difficult to evaluate because there is no spacer between the GaAs substrate and the graphene. For samples on silicon the oxide layer is usually chosen to be 90nm or 280nm to make the graphene visible to the naked eye. On our samples we were unable to see the graphene directly. Under an optical microscope we were only able to see the edges of the graphene where it was dirty or rolled up.

We attempted to get a better idea of the coverage using scanning electron microscopy (SEM). An SEM secondary electron image can show the graphene with better contrast than optical microscopy. The main obstacle we encountered was the need to image large areas. The Raith 150 electron beam lithography system in ExFab, which we used as an SEM for this project, gave images with nonuniform brightness in the lowest-magnification settings of the in-lens detector, and imaging of the entire sample required manual stitching of the images. It may be possible to use different settings to make this more practical but we did not attempt this. We also did not attempt to take Raman maps because of time constraints.

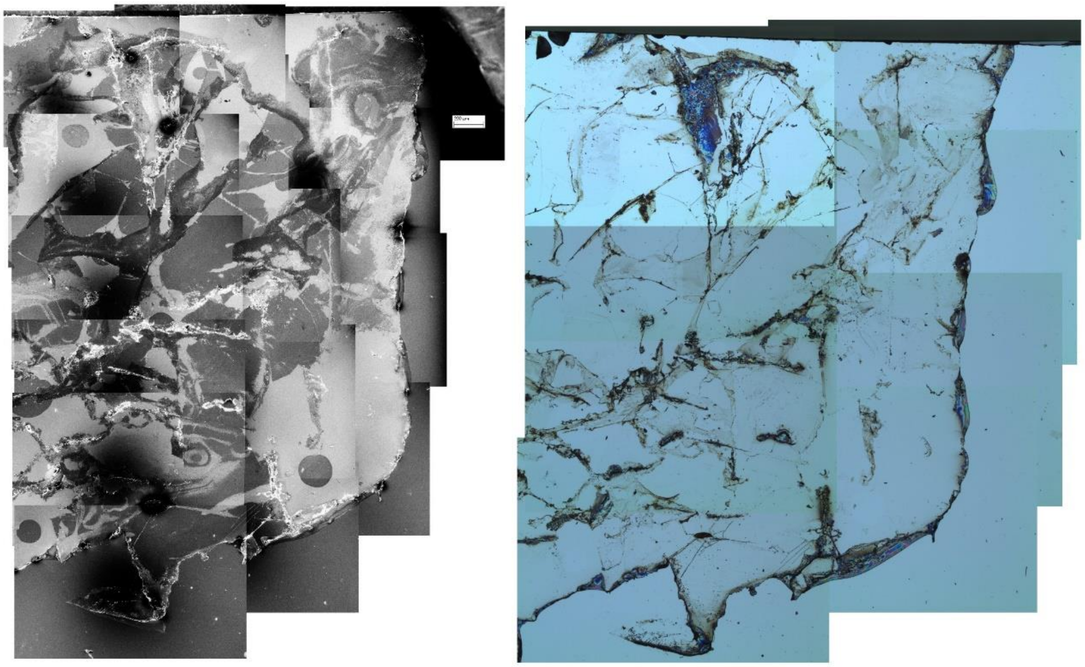

Figure 14. Stitched Raith SEM and optical microscope images of sample G1D (early attempt to transfer) showing large number of tears and discontinuous graphene regions. Scale bar in SEM image is 200µm.

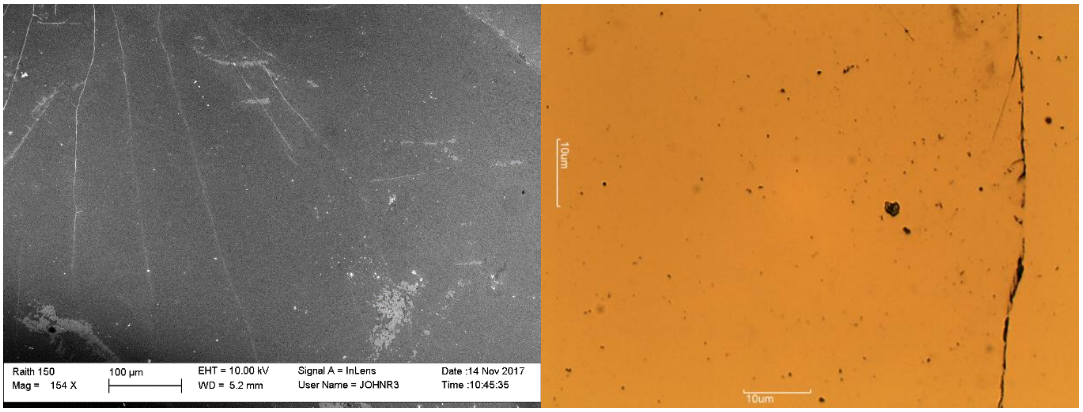

Figure 15. Raith SEM optical microscope images of sample G2C showing coverage improved by reducing wrinkles to copper foil. Areas without graphene are visible in the upper right corner of SEM image and right edge of optical microscope image

We found that by minimizing the wrinkles in the copper foil we were able to significantly improve the graphene coverage (figure 15) so that there were large (hundreds of microns) continuous areas. However after this improvement we did not focus on graphene coverage because it became apparent that residues were more limiting to the MOCVD growth process. We also found that within the visible boundaries of the graphene, randomly selected points almost always gave Raman spectra indicating graphene, another sign that the coverage was adequate (i.e. that there were no large tears that we could not see by eye under an optical microscope).

Figure 16. Samples G4AB (left, with thick 200nm PMMA) and G4CD (right, with thin 50nm PMMA) on GaAs during transfer, before drying, showing the visible difference between thick and thin PMMA. Thick PMMA appears to have more wrinkles.

As a result we did not determine whether coverage is better for transfers using thick or thin PMMA, or for baked or unbaked PMMA. By eye, the thin PMMA generally looks better before it is removed (figure 16). This may be a sign that thin PMMA gives better graphene coverage, but it would be much easier to study this effect using graphene transferred to silicon wafers with an oxide spacer.

We also used optical microscopy to diagnose our problems with contamination caused by the new batch of copper etchant for several rounds of transfer, as we discuss below.

5. Annealing and characterization

Before the MOCVD growth, the adhesion between graphene and GaAs substrate was improved. To encourage the atomic registry between subsequent GaAs MOCVD epi-layer and substrate, it is necessary that the graphene conform well to the surface of the substrate. To increase the adhesion, all samples were annealed in ambient H_2 and N_2 under 350C for 30 minutes, following Y. Kim *et al*. We used the All-Win 610-r in SNF.

To characterize the annealing, we split a graphene/GaAs sample, annealed one half, and measured the surface roughness of both parts. In figure 17, the surface roughness was high without annealing and decreased by a factor of two with annealing. The results are summarized in the table below. The roughness of graphene was almost the same as the GaAs substrate after annealing, which suggests that the annealing improves the conformity of graphene. [19]

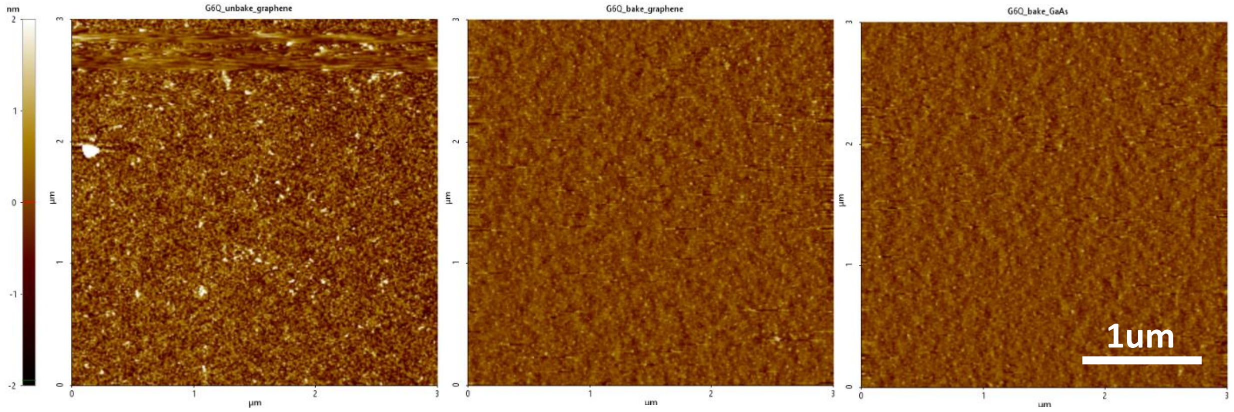

Figure 17. The AFM images of (Left) graphene/GaAs before annealing, (Middle) graphene/GaAs after annealing and (Right) bare GaAs after annealing. All three images have the same length scale. The color scale is from -2 to 2 nm.

	Before Annealing - graphene	After Annealing - graphene	After Annealing - GaAs
Roughness(nm)	0.54	0.28	0.27

Table. RMS surface roughness before and after annealing.

We took Raman spectra of the graphene on the annealed and not-annealed halves of the sample (figure 18). The annealed half of the sample had a slightly large G peak (G/2D = 0.45) compared to the half that was not annealed (G/2D = 0.30), and the G and 2D peaks were blue-shifted by $1cm^{-1}$ and $3.5cm^{-1}$, respectively. The small blue shifts indicate compressive strain or doping by holes [19], although these effects are not as large as sometimes reported in the literature (reference [19] estimates that a $10cm^{-1}$ shift corresponds to doping around $1x10^{13}cm^{-2}$). The defect peak is comparable with and without annealing indicating that the graphene is not heavily damaged by annealing.

---

[19] Z. Cheng *et al*., 'Towards Intrinsic Graphene Surfaces: A Systematic Study of Thermal Annealing and Wet-Chemical Treatment of SiO_2-supported Graphene Devices', Nano Lett. **11**, 767-771 (2011)

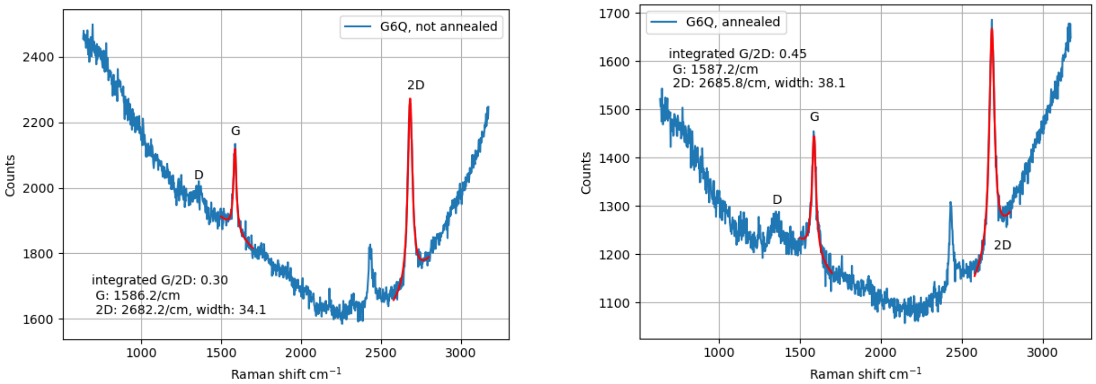

Figure 18. Raman spectra of graphene that is not annealed (left), and graphene from the same sample that has been annealed (right) with fit parameters showing blue shifts of G and 2D peak and larger G peak.

6. MOCVD GaAs Growth

Metal Organic CVD is a high flexible process that can deposit semiconductors, metals and dielectrics. [20] MOCVD utilizes metal organics and hydrides as precursors. Near the substrate surface, the precursors gases are decomposed, and the target material are deposited. In SNF, the Aixtron 200 reactor is a specialized tool for depositing III-V materials using MOCVD process. It has horizontal flow design and rotating stage to ensure the uniformity of growth.

The precursor for GaAs growth are tertiarybutylarsine (TBAs) and Trimethylgalium (TMGa). The process can be divided into two parts:

- Nucleate for 100nm with good density
- Growth for 1.5um for planarization

The following are the parameters we have tuned:

- Growth time
- Growth temperature
- V-III precursor ratio
- Carrier gas

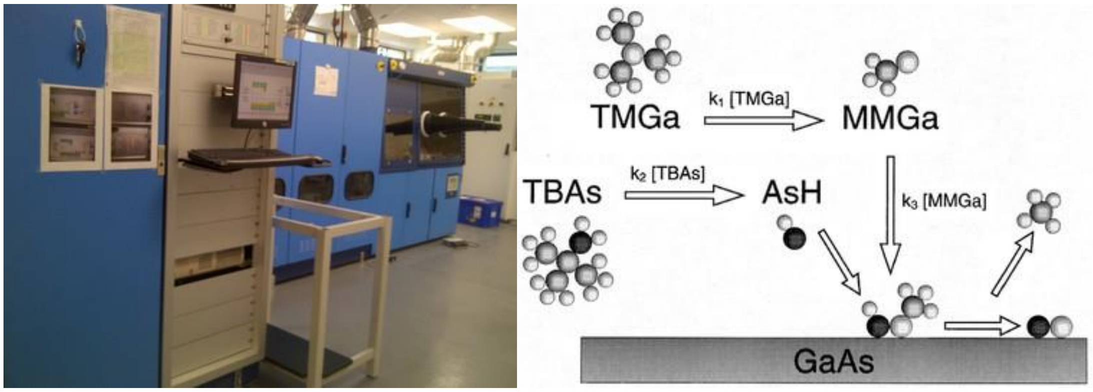

Figure 19. Aixtron 200 reactor and a schematic of MOCVD process for GaAs growth, from [21].

---

[20] SNF MOCVD lab capability introduction, aix200: https://snf.stanford.edu/SNF/equipment/chemical-vapor-deposition/mocvd/aix200

[21] O Féron et al., Applied Surface Science 159–160 (2000) 318–327

7. Characterization of MOCVD growth

7.1. Initial Attempts of Full Growth

Figure 20 shows the SEM image of a full MOCVD growth after we obtained a sample with large area graphene. MOCVD parameters:

- Nucleation: 10 min, 450C, V/III ratio=100sccm/10sccm
- Growth: 30 min, 650C, V/III ratio=100sccm/10sccm

The region in SEM image is the boundary of graphene-uncovered and covered region. The growth can be understood more easily using the illustration in figure 20 right. Before the growth, graphene covered the GaAs substrate on the right part, while GaAs substrate is exposed on the left part.

During the MOCVD process, in the exposed GaAs area, the precursors nucleated and grew very well because epitaxy of GaAs on GaAs is easy. But in the graphene-covered area, the epitaxy is less trivial because it requires high quality and optimal growth condition. If it grew well, we expected to see about 1 um of GaAs epi-layer on graphene which was obvious not the case. It only showed rough islands of GaAs in this region.

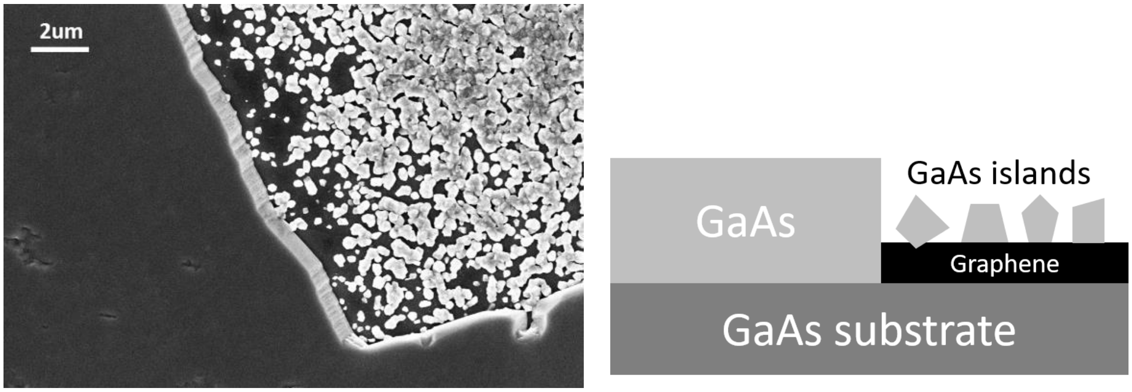

Figure 20. (Left) SEM image of GaAs growth on graphene/GaAs. (Right) An illustration of the cross-section of the sample.

7.2. Characterize the nucleation

To troubleshoot the growth, we conducted only nucleation. The MOCVD parameters are:

- Nucleation: 10 min, 450C, V/III ratio=100sccm/10sccm

The nucleation turned out to be non-ideal. Good nucleation sites should be sparse GaAs plateaus. Instead, the sample was covered by dense nanowires (Fig. 20 left). In the area without graphene, there are pits and sparse nanowires (Fig. 20 right). The pits possibly came from the holes created by HCl in the oxide stripping step.

In order to grow a high quality epi-layer and ensure the registry between GaAs nucleation and underlying GaAs, nanowires need to be removed. There are three possible ways the to suppress the growth of nanowires:

- High growth temperature

- High V/III flow rate
- Reduce metallic residual

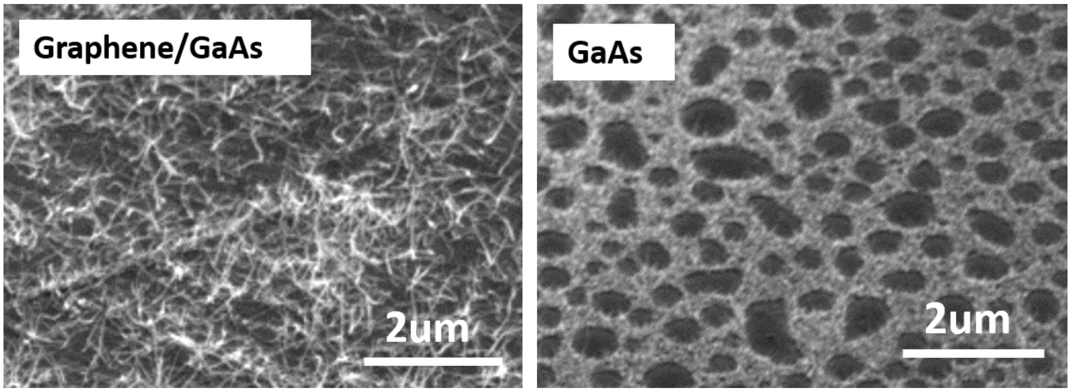

Figure 21. SEM images of nucleation on (Left) the graphene-covered area (Right) exposed GaAs area. (sample G4)

7.3. Attempt to suppress nanowires

7.3.1. High temperature nucleation

It is known that nanowires are not preferred in high temperature, so we conducted nucleation at a slighter higher temperature.

- Nucleation: 10 min, 500C, V/III ratio=100sccm/10sccm

Nucleating in higher temperature, we did remove the nanowires. Yet, there was still no plateau-shape of nucleation. Most of the nucleation sites still had irregular shapes. We tried to use a slower rate by reducing the flow rate and increase the growth time, but it did not improve. Even under 1 hour of nucleation, the sites were still irregular, and the density did not change accordingly. It was possibly because, with high thermal energy, the precursors tended to diffuse around the surface, so they still went to those sites and formed irregular nucleation.

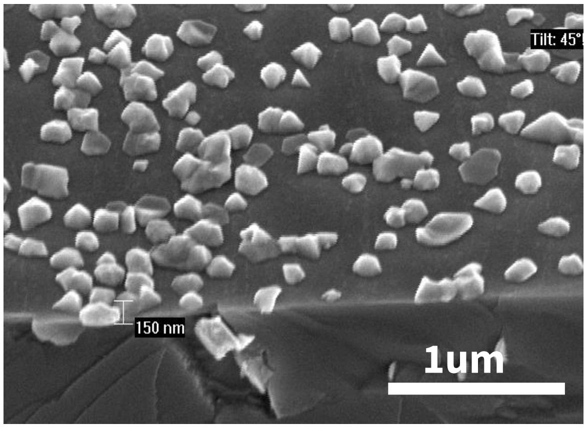

Figure 22. SEM image of nucleation on graphene-covered region. (sample G4K)

7.3.2. Attempt to suppress nanowires: high V/III ratio flow

One study found that GaAs nanowires are formed in MBE growth because of gallium droplets on substrate surface [22]. High As/Ga ratio can decrease the gallium droplets and, thus suppress the formation of nanowires. [23]

- Nucleation: 10 min, 500C, V/III ratio=150sccm/10sccm

The result went opposite to the expectation. The density of nanowires was even higher than the nucleation under low V/III ratio. The reason might be that we used metal organic precursors, in contrast to the paper in which they used Ga and As flux under MBE method. [21] Their results might not apply to ours directly.

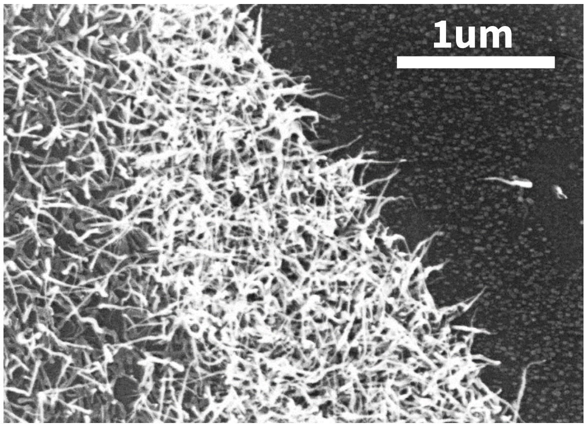

Figure 23. SEM image of nucleation. On the left part of the image is the graphene-covered region, while the right part is the exposed GaAs region. (sample G6H)

7.3.3. Attempt to suppress nanowires: reduce contamination, increase etch time

It is known that metallic residuals or other contaminations can act as catalysts and encourage the growth of nanowires. Figure 24 shows the OM image of graphene. One of the features is that there are long, thin lines in the sample, which might come from the wrinkles or folding of graphene. There are also short, thick stain-like patterns which might be the contaminations that caused nanowires.

---

[22] Katarzyna Gas et al., Nanoscale, 2013, 5, 7410 (2013)

[23] Yazeed Alaskar et al., Adv. Funct. Mater. 2014, 24, 6629–6638 (2014)

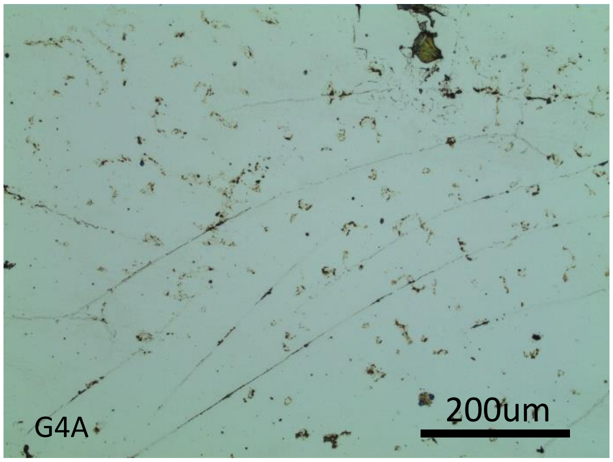

Figure 24. Optical microscope image of graphene on GaAs.

Our first guess about those patterns was that they were the residuals of the copper foil. To remove them, we tried to leave graphene/Cu in copper etchant solution longer. We increased the copper etching time to 2 hours, 4 hours and 12 hours. The OM results showed that the quality of graphene did not correlate with etching time (Figure 25). After nucleation, all samples had nanowires and their density did not correlate with etching time. For example, 4 hours of etching produced lower density while the 12 hours had the highest density.

- Nucleation parameters: 10 min, 450C, V/III ratio=100sccm/10sccm

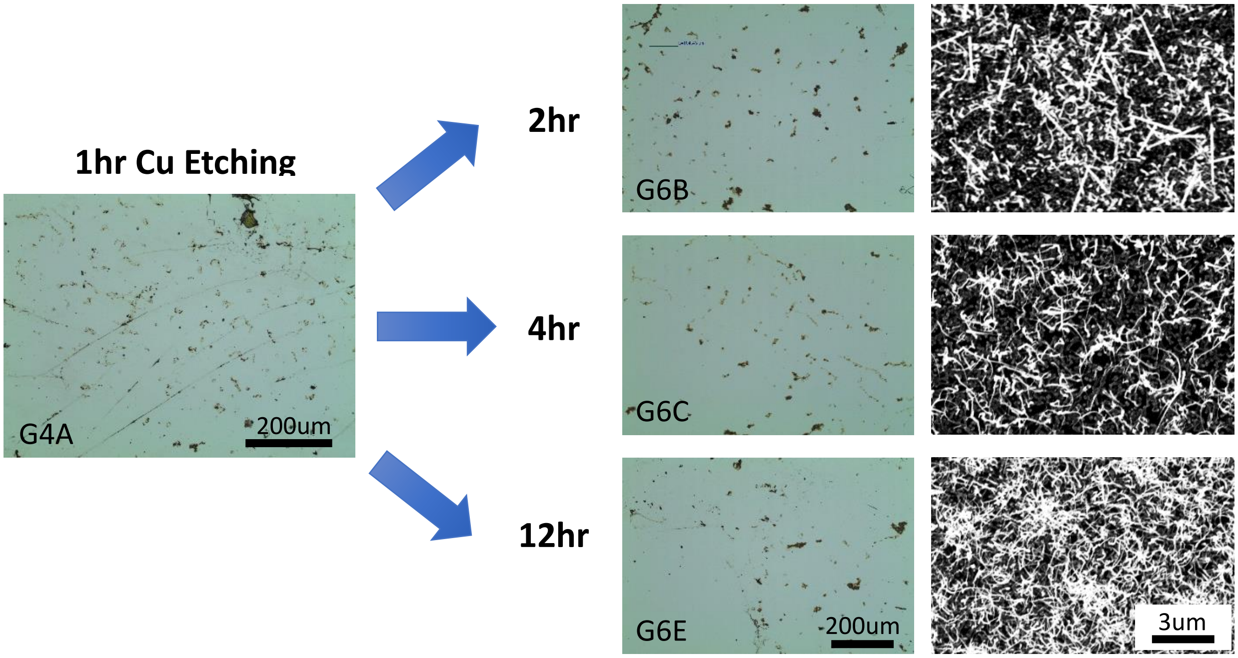

Figure 25. (Left) OM image of graphene on GaAs. (Right) OM images of graphene on GaAs and SEM images of GaAs-grown graphene/GaAs.

7.4. Reduce contamination

7.4.1. Different etchant batch

Since the metallic contamination was unlikely to come from copper foil residual, the only other metallic source was the copper etchant. We had ordered a new batch of copper etchant, and the appearance of the contamination turned out to coincide with the first use of the new etchant. So we switched to a previously-opened, expired bottle of etchant. With this different bottle, the patterns became invisible under OM. We are not sure what component caused those patterns. When we used our newly ordered etchants, there were always patterns. But after switching to older etchants in chemical stockroom, we had never seen the problem again.

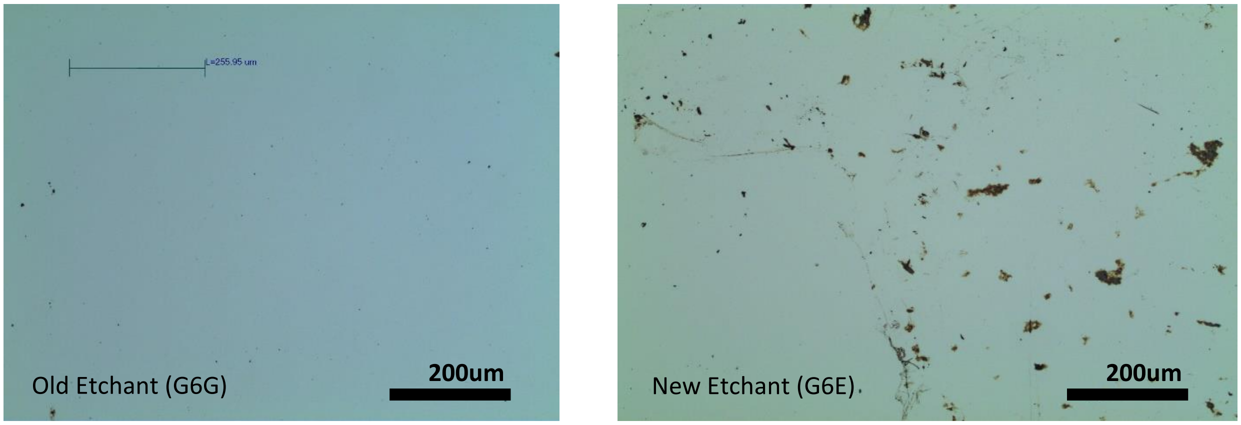

Figure 26. OM images of graphene on GaAs. (Left) Old and (Right) New etchant were used in copper removal.

With a clean sample like figure 26, left, we attempted the nucleation again.

- Nucleation: 10 min, 450C, V/III ratio=100sccm/10sccm

The result improved quite a lot. The nanowire density decreased drastically, and we could see small nucleation sites on the sample (figure 27, left). However, most of the sample were still covered by nanowires (figure 27, right). The contamination needed to be reduced even further.

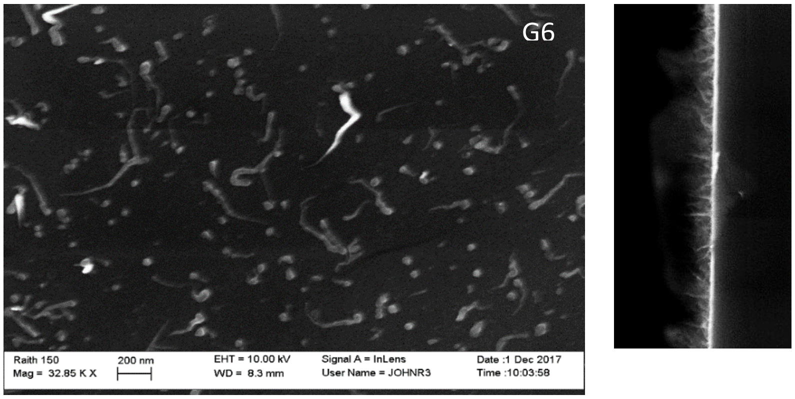

Figure 27. SEM images of nucleation on clean sample. (Left) Top view. (Right) Cross section.

7.4.2. More water baths in graphene transfer

To characterize the elemental component of the contamination in the sample, we conducted Auger spectroscopy. Figure 28 shows Auger spectra at two different locations of a sample (red and blue lines). Besides Ga, As, C and O, whose existence we already knew, there were very weak signals from Cu and Cl. This suggested that there might be residuals from the copper etching step. To reduce the reduce the residuals, we doubled the number of DI water cleaning baths from 4 to 8 in the graphene transfer process.

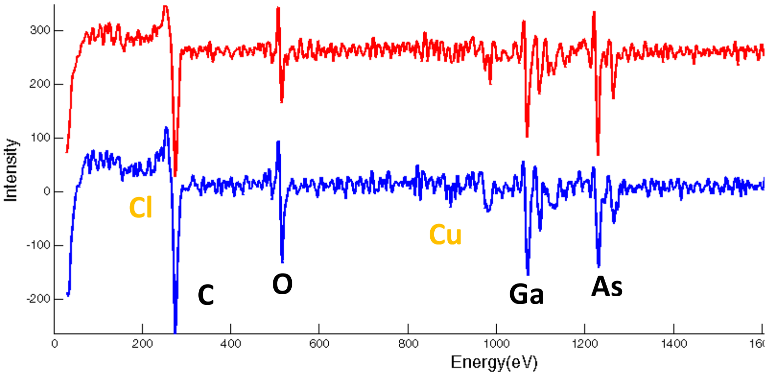

Figure 28. Auger spectra at two different locations of a sample.

With this cleaner transfer procedure, the nucleation improved. Although there are still quite some regions that had many nanowires (figure 29, upper left), there are some regions that had almost no nanowires (figure 29, lower left and right). Note that the density and thickness of the nucleation was still too low.

- Nucleation: 10 min, 450C, V/III ratio=100sccm/10sccm

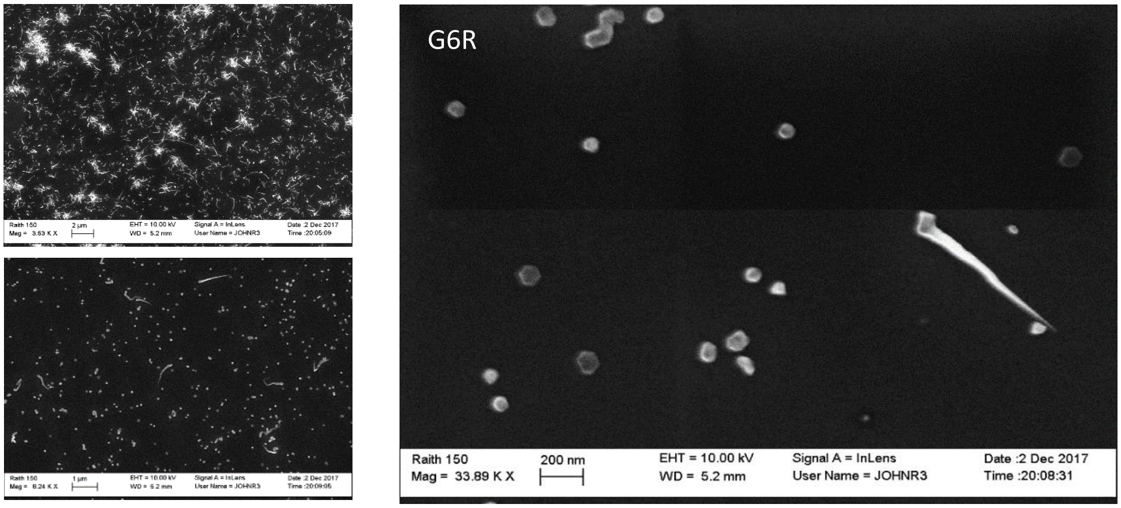

Figure 29. SEM images of nucleation on the sample using more DI water bath. (Upper Left) Bad part of the sample. (Lower Left) Good part of the sample. (Right) Zoomed-in of the good area.

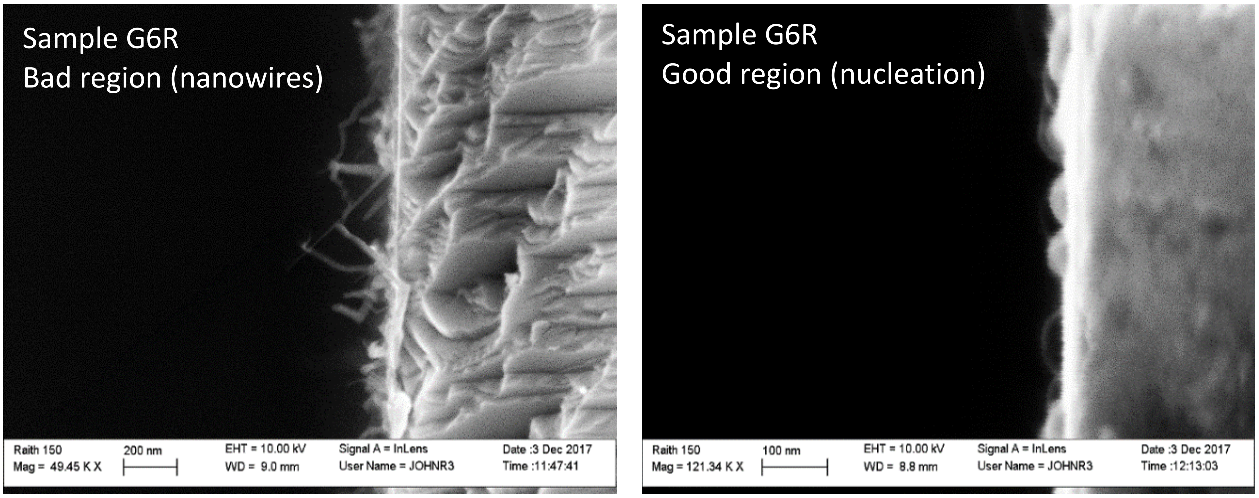

Figure 30. Cross-section views of SEM images on the sample as in figure 29. (Left) Bad part of the sample. (Right) Good part of the sample.

7.5. Longer nucleation time and full growth on clean sample

To increase the nucleation density and thickness, we used an extended nucleation time.

- Nucleation: 60 min, 450C, V/III ratio=100sccm/10sccm

Much of the sample was still covered in nanowires, but some areas show clean nucleation (figure 31). The density increased by about two- to three-fold. The thickness also increased to 100-200 nm.

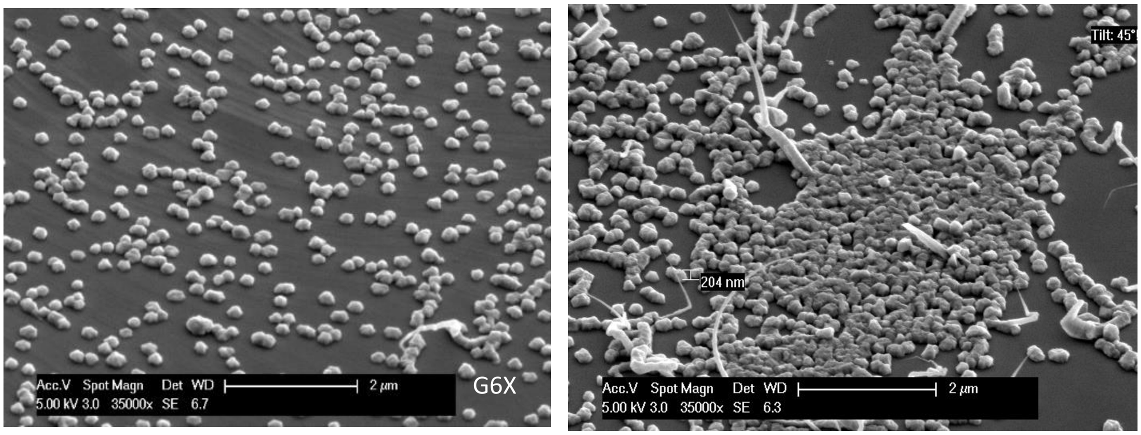

Figure 31. SEM images of regions of good nucleation on clean samples, 45 degree tilt

With this result, we conducted a full growth. The result is shown in figure 32. Although the sample did not planarize completely into a good surface, there were also good regions and bad regions. In figure 32, middle, the growth formed rod-like structure. While in figure 32 right, different nucleation sites connected into almost a continuous layer.

- Nucleation: 50 min, 450C, V/III ratio=100sccm/10sccm
- Growth: 50 min, 650C, V/III ratio=100sccm/10sccm

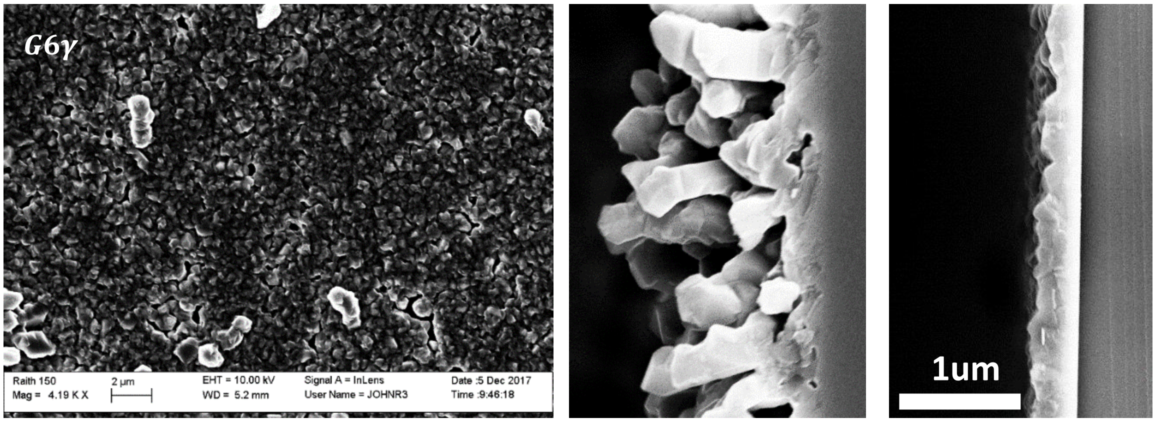

Figure 32. SEM images of a full growth. (Left) Top view. (Middle) Cross section of bad area. (Right) Cross section of good area.

To characterize the crystallinity of the GaAs epilayer, we conducted electron back-scatter diffraction (EBSD) to see if the crystallinity agreed with the underlying substrate. Figure 33 left shows that the EBSD was measured in a good region like figure 32 right. The EBSD map shows that the epilayer is polycrystalline with many of the islands having (001) or (111) orientation (figure 32 upper right). The substrate is GaAs(100), which appears to be uniformly red under EBSD (figure 32 bottom right). It is possible that parts of the epilayer are aligned with the substrate but we would be unable to distinguish this case from random orientations.

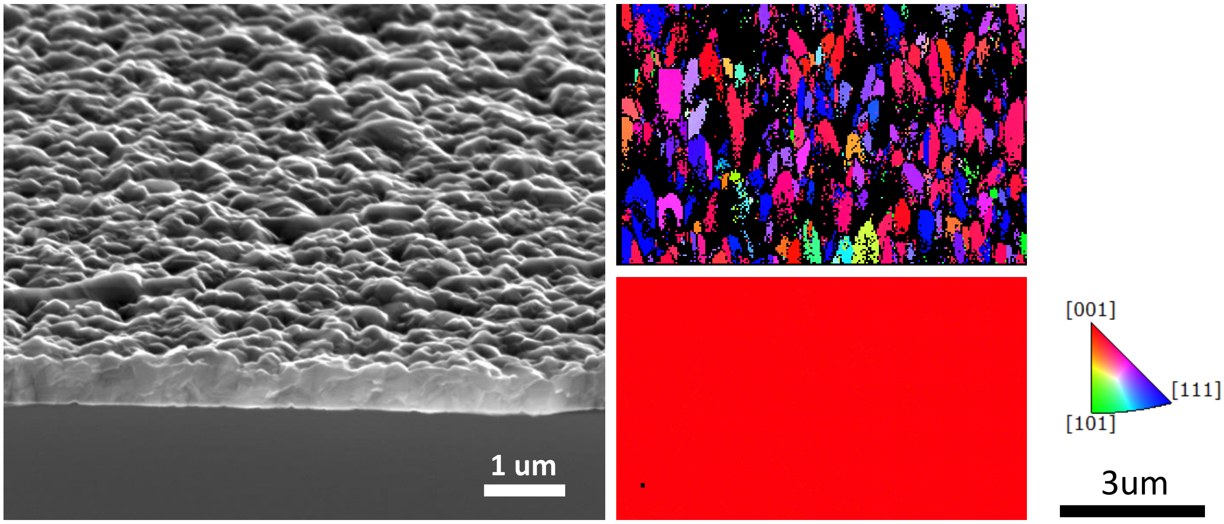

Figure 33. (Left) 45 degrees SEM images of the good region of epi-layer. (Right) EBSD map of the (Top) same region and (Bottom) outside of graphene-covered area. Note that we took an EBSD map on the rough top surface of the epilayer while Y. Kim *et al.* use the smooth underside after exfoliation.

7.6. H_2 carrier gas

We had also tried using a different carrier gas. Typically, the growth of III-V semiconductors including GaAs uses H_2 as carrier gas. However, in Y. Kim *et al* use N_2 instead, to prevent the decomposition of graphene in H_2 at high temperature. In this experiment, we used H_2 to see if H_2 could remove contamination and assist the nucleation.

- Nucleation: 10 min, 450C, V/III ratio=100sccm/10sccm
- Carrier Gas: Hydrogen

The results are shown in figure 34. On a single sample, there were still good regions and bad regions. In the bad region (figure 34 left), some nanowires could be seen. But their density was much less than before. In the good region, there was almost no nanowire. Note that this nucleation only took 10 min, but it got comparable density to 1 hour nucleation. Interestingly, between good and bad regions, there were intermediate regions. In figure 34 middle, nanowires were few and only showed up as discrete packs. There were high density of nucleation sites in this region. These sites lined up in parallel patterns (figure 35 left). It is possibly due to the wrinkles from the transfer process.

Figure 36 shows the nucleation at the boundary of graphene-covered and exposed GaAs region. In the exposed GaAs region, an almost flat epi-layer was formed, while a lot of nanowires emerged at the boundary. This is possibly because there were more contaminations trapped in the boundary due to the wrapping of graphene, so nanowire growth was preferred here.

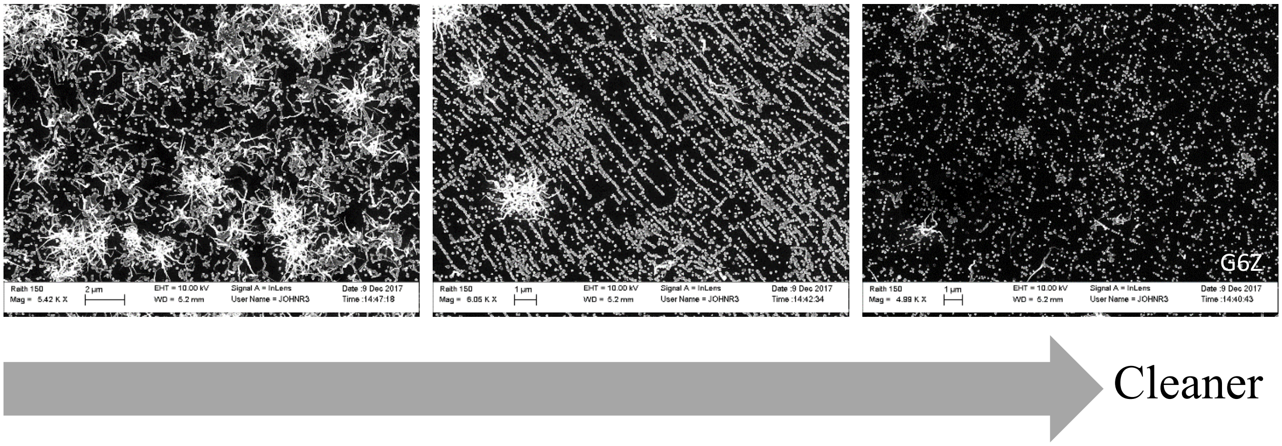

Figure 34. SEM images of nucleation. From left to right are contaminated regions to clean regions on the same sample.

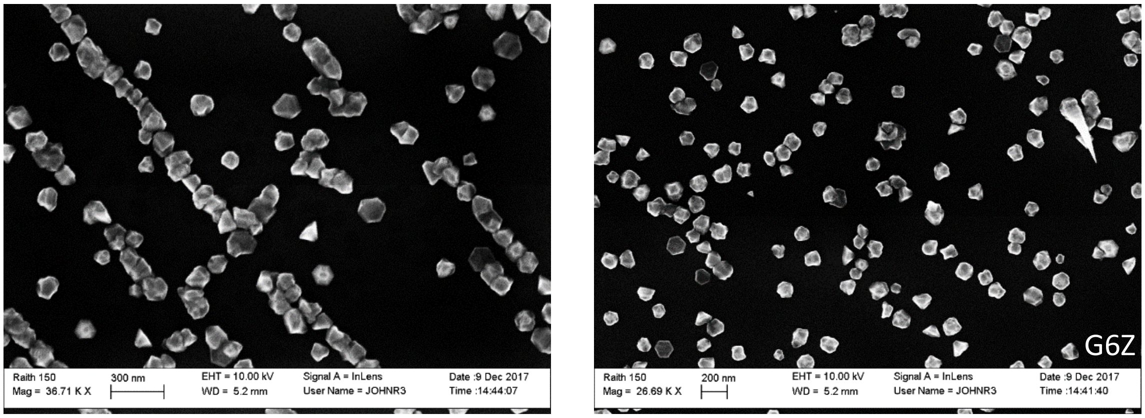

Figure 35. Zoomed-in SEM images of nucleation. (Left) The region from figure 34 middle. (Right) The region from figure 34 right.

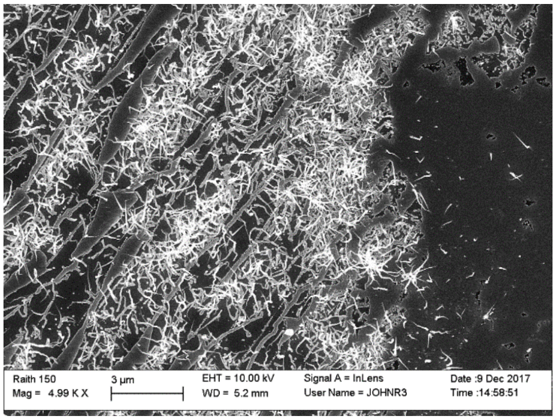

Figure 36. SEM image of nucleation at the boundary of graphene-covered area. Graphene covered the left of this figure, while GaAs was exposed on the right.

8. Exfoliation and characterization of the GaAs epilayer

8.1. Exfoliation procedure

The final step of the process is mechanical exfoliation of the grown GaAs epilayer from the substrate. It should be possible to remove the epilayer regardless of whether it is epitaxially registered to the substrate. We performed an exfoliation on one sample (G6γ, another part of the same sample on which we performed EBSD measurements).

Figure 37. Left: Sample G6γ mounted on the AJA chuck before evaporation (sample on the right), showing the as-grown surface after MOCVD. The rougher region (outlined in red) is the graphene area. **Center:** After deposition of the Ti/Ni stressor layer (a problem with the evaporator required the samples to be unloaded and mounted again). **Right:** Substrate and the exfoliated epilayer immediately after the tape is peeled off. Area on the left part of the tape corresponds to the graphene region.

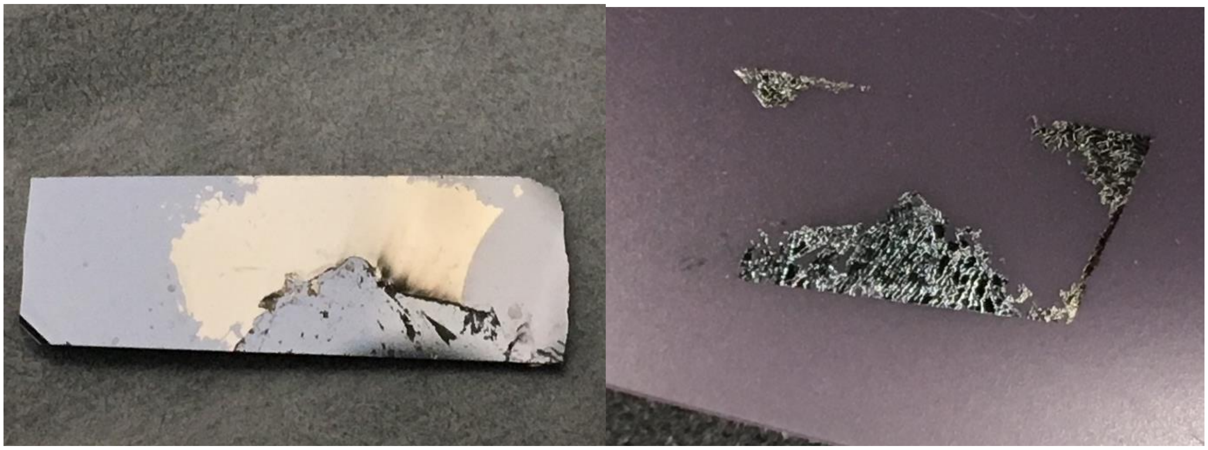

Figure 38: Substrate (left) and epilayer on thermal release tape (right) after exfoliation.

The exfoliation is preceded by deposition of metal films intended to cause stress at the graphene-epilayer interface according to Y. Kim *et al*. We used the AJA electron beam evaporator in ExFab to deposit a 100nm titanium adhesion layer (2.0Å/s) followed by a 180nm nickel stressor layer (1.0Å/s). We then applied thermal release tape (TRT) to the surface of the sample and peeled it off with tweezers. The epilayer released in the graphene region, with large areas revealing a smooth surface that appeared to be the original GaAs wafer surface (figure 37-38). Under an optical microscope (figure 43), the graphene region of the substrate appears to have spots where the GaAs/stressor layers did not exfoliate. The exfoliated epilayer appears mostly spotted with some clear regions.

8.2. Raman spectroscopy and optical microscopy

We performed Raman spectroscopy on the substrate and on the bottom of the epilayer (still on TRT). Two of three locations in the graphene region of the substrate showed both the G and 2D peaks. One showed the G but not 2D peak. The G peak appeared larger than the 2D peak, which could indicate doping or strain caused by the MOCVD growth process.

Of seven locations in the epilayer, three showed no signs of graphene (one in the clear region and two in the spotted region), while four (all in the spotted region) showed G and 2D peaks. It appears that the graphene that stuck to the epilayer was not doped or strained like the graphene remaining on the substrate. Graphene may have stuck to the epilayer because the adhesion to the substrate was generally not good, which could also be responsible for the polycrystallinity of the epilayer (the adatoms did not interact with the potential of the substrate because the graphene did not adhere tightly to the substrate). A more thorough Raman map should be taken of the samples to quantify the graphene adhesion.

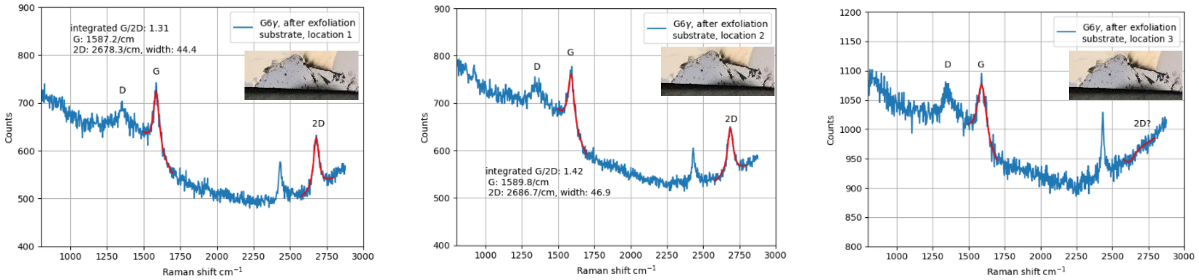

Figure 39. Raman spectra of three locations in the graphene area of the exfoliated substrate, two of which show both G and 2D peaks.

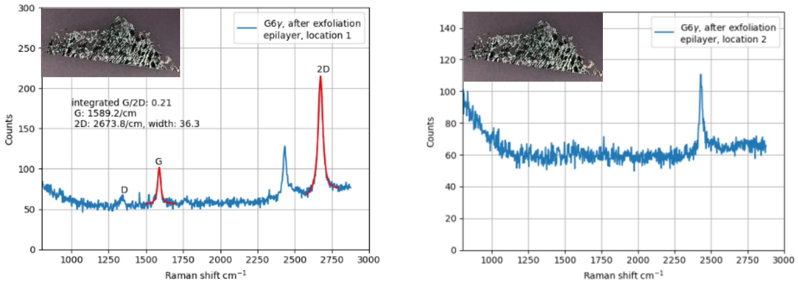

Figure 40. Raman spectra of two locations on the underside of the epilayer, one of which shows graphene G and 2D peaks. Of five additional locations not shown here, three showed graphene and two showed no graphene.

We extended the range of our Raman spectra to include the GaAs peaks around 300cm^{-1}. All three locations on the substrate show a normal GaAs Raman spectrum, while all seven locations on the epilayer, in addition to what is likely the GaAs LO phonon peak, show another peak around 270cm^{-1}. This is likely a TO phonon peak known to appear as a surface mode in the Raman spectra of GaAs samples that are porous or defective. [24][25] This indicates a defective GaAs layer which is confirmed by SEM (below). This makes sense given the nonuniform growth especially in regions dominated by nanowires during nucleation. Since most of the epilayer released it appears that the good and bad regions both detached from the substrate. Both spotted and relatively clear regions show the forbidden GaAs TO phonon peak indicating defects (although we may not have taken Raman data on the least defective regions).

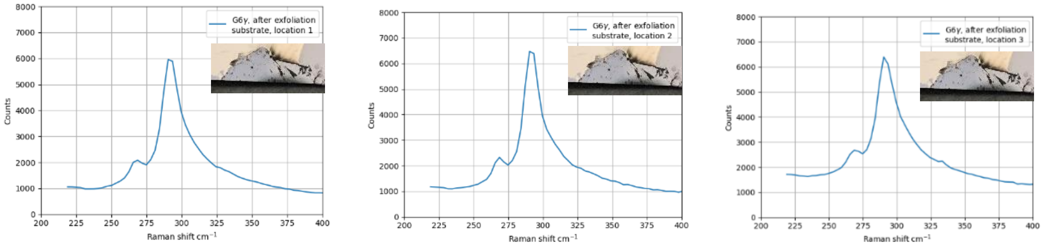

Figure 41. Raman spectra of three locations on substrate showing GaAs phonon peaks.

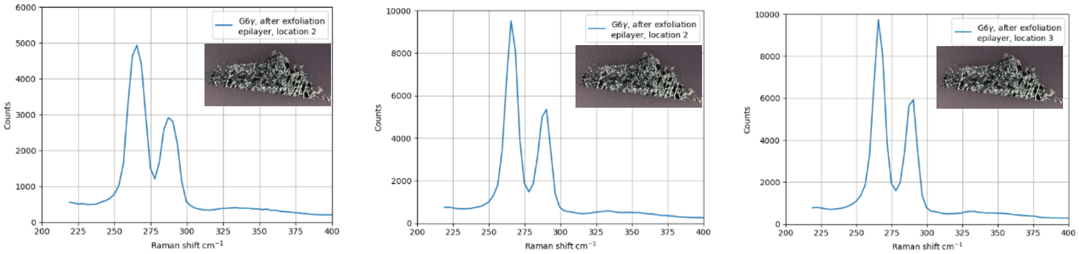

Figure 42. Raman spectra of three locations on the epilayer showing what appears to be the GaAs phonon peak and another, lower-energy peak.

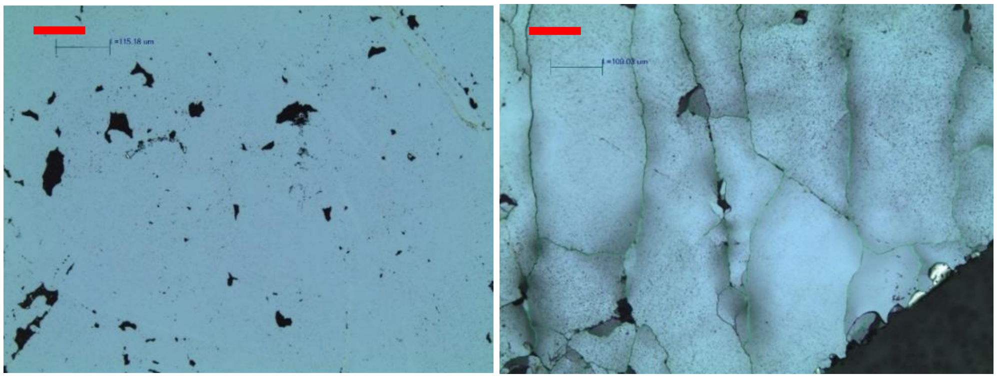

Figure 43. Optical microscope images of the substrate graphene region after exfoliation (left) and the bottom of the epilayer (right) on thermal release tape. Red scale bars 100μm.

---

[24] M. Tiginyanu *et al.*, 'Porosity-induced modification of the phonon spectrum of n-GaAs', Semiconductor Science and Tech. **12** (4), 491 (1997)

[25] Y. Alaskar *et al.*, 'Towards van der Waals Epitaxial Growth of GaAs on Si using a Graphene Buffer Layer', Adv. Functional Mat. **24** (42), 6629-6638 (2014).

8.3. SEM and EBSD characterization

We used SEM/EBSD measurements to characterize the underside of the exfoliated epilayer. This was a difficult measurement because our layer was too thin to remove from the thermal release tape, so we placed the sample on tape into the SEM. This resulted in charging which we were able to mitigate by making a silver paint contact to the epilayer. In addition, the tape melted under the electron beam, and since the sample was mounted at a high angle this caused the entire sample to slide downwards at times. This may be responsible for the poor EBSD signal. The appearance of the surface varied from pitted to smooth (figure 44). The pitted regions appeared to correspond to the spotted regions under OM, but even some regions that appeared smooth under OM were still more pitted than the best parts of the epilayer (so we can't draw conclusions about how large the smooth regions are based on OM).

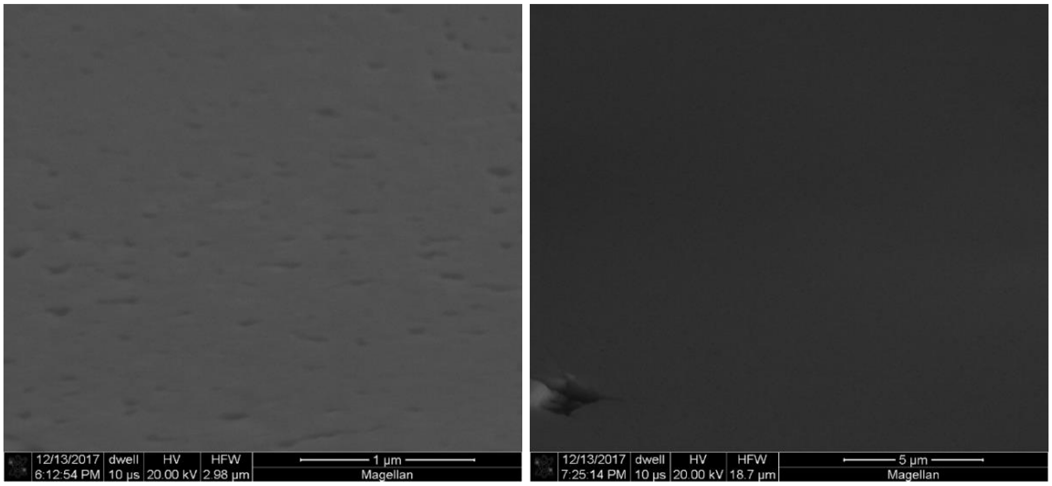

Figure 44. SEM images of the underside of the epilayer taken during EBSD measurement, showing parts of the pitted region (left) and smooth region (right).

We took EBSD maps at seven points on the epilayer (figures 45-47). The more pitted regions showed random orientations in all three planes. Smoother regions showed preferential out-of-plane alignment to the [111] direction. The in-plane alignment tended to vary, but show a consistent alignment over microns (larger than the grain sizes in the pitted regions). The random orientations in the pitted areas are consistent with the results from Y. Kim *et al.* when there is no registry to the substrate. A possible explanation is that in the polycrystal region, the nucleation was not done very well so the orientations are not uniform, possibly due to defects, surface morphology or contaminations.

The occurrence of GaAs (111) face instead of (001) indicated that the remote registry likely did not work, possibly because of the weak adhesion of graphene to substrate or trapped residuals between graphene and substrate. In the smooth region, it might be that the nucleation happened at a cleaner region, so it developed into a more uniformly oriented film. The (111) growth is consistent with the hexagonal nucleation sites that we observed while characterizing the MOCVD growth (figure 29). The in-plane EBSD maps indicate that our epilayer is not single-crystalline. Instead it appears to be composed of domains that are rotated in the plane while maintaining out-of-plane alignment to the [111] direction.

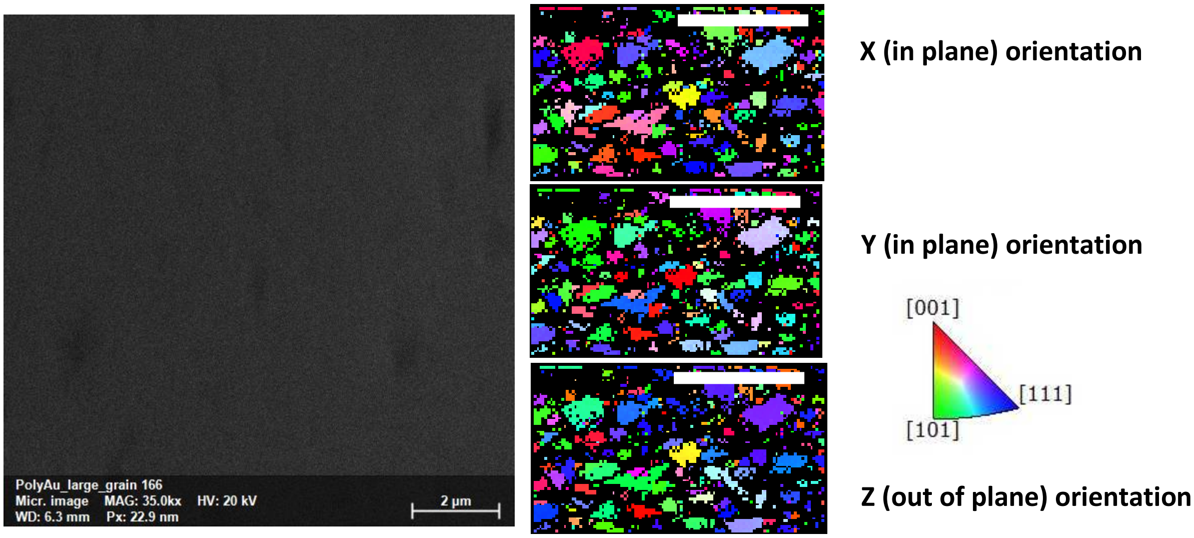

Figure 45. SEM image of a pitted region on the underside of the epilayer, and EBSD map of part of the region showing random orientation. EBSD scale bar 1µm.

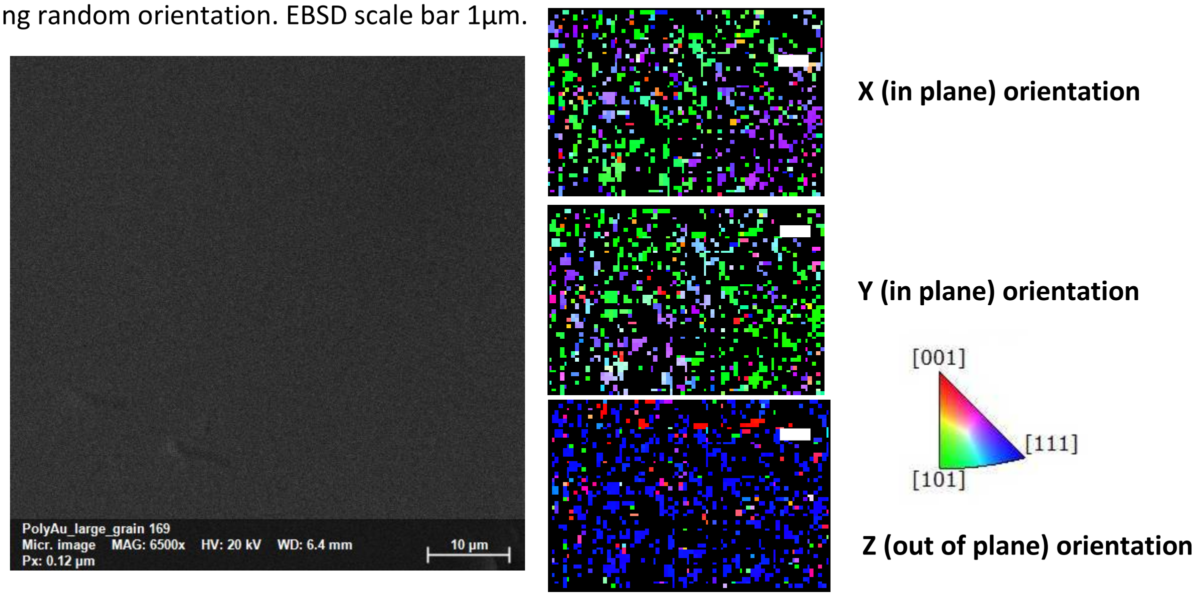

Figure 46. SEM image of a smooth region on the underside of the epilayer, and EBSD map of part of the region showing that the out-of-plane alignment is preferentially (111). EBSD scale bar 1µm**.**

The mechanism responsible for [111] alignment is uncertain. The reason that (111) was preferred over (001) or (011) could be related to the fact that surface energy of (111) is lower than that of other orientations [26][27]. For GaN growth on graphene/SiC, an aligned epilayer can be caused by surface features such as steps [28], but we do not seem to have features that could cause aligned nucleation. A likely explanation is that the (111) orientation could be imparted by the graphene. It has been shown that in low-temperature MBE growth of thin GaAs on Ga-terminated graphene/silicon, the hexagonal

---

[26] C. Messmer, 'The surface energy of Si, GaAs, and GaP', *Journal of Applied Physics* **52**, 4623 (1981).

[27] N. V. Sibirev, 'Surface Energy and Crystal Structure of Nanowhiskers of III–V Semiconductor Compounds', *Physics of the Solid State* **52** (7), 1531–1538 (2010).

[28] J. Kim *et al*., 'Principle of direct van der Waals epitaxy of single-crystalline films on epitaxial graphene', *Nat. Comm.* **5.** Article number 4836 (2014), DOI: 10.1038/ncomms5836

lattice of the graphene can cause (111) GaAs growth. [29] This could occur despite the lattice constant mismatch between GaAs/graphene because of an aligned supercell of multiple unit cells.

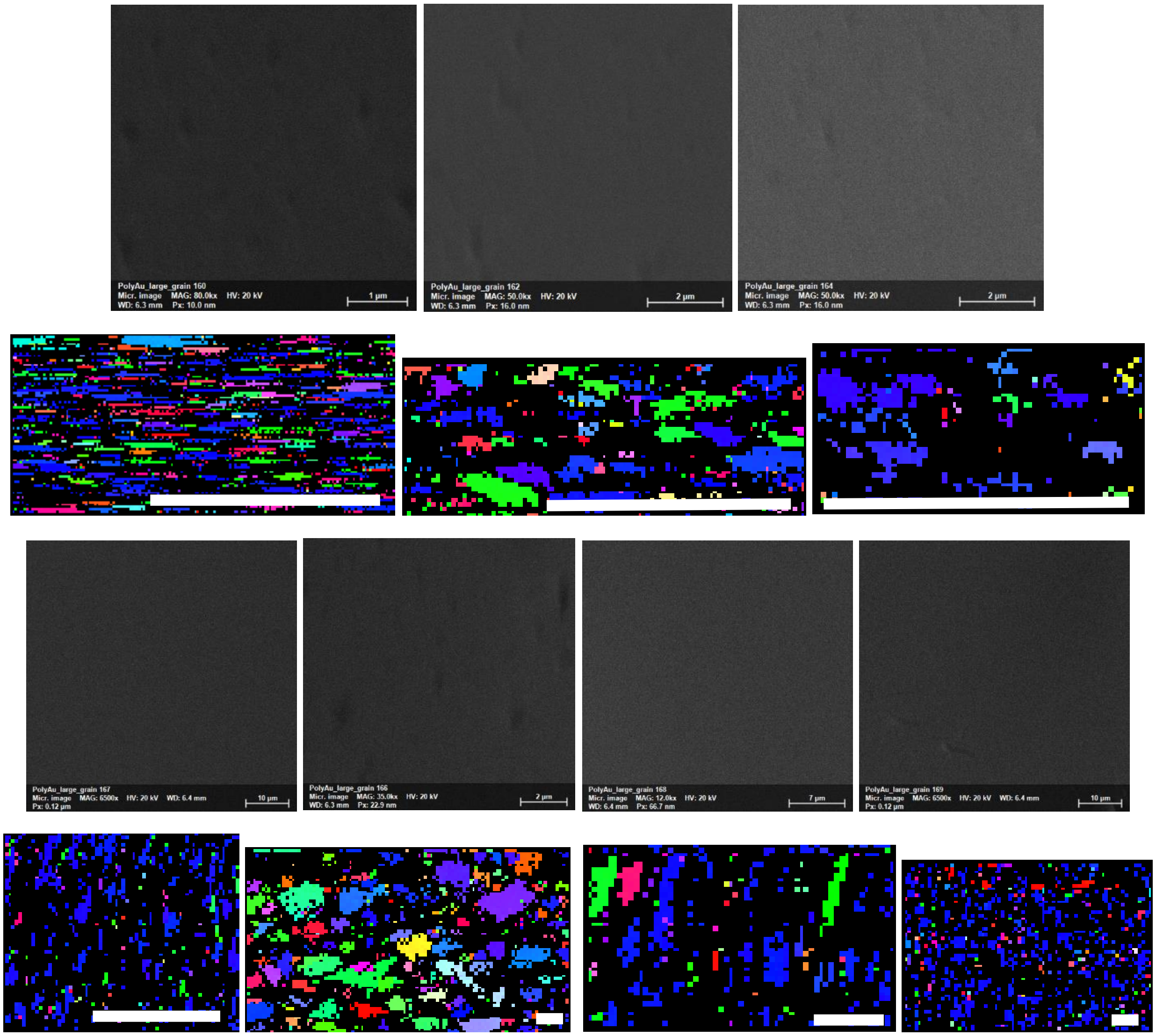

Figure 47. All locations on the epilayer at which we took EBSD maps, showing only the out-of-plane (z-) maps and the SEM image of the region where the map was taken. EBSD key is the same as above. All scale bars are 1µm.

---

[29] Y. Alaskar *et al.*, 'Towards van der Waals Epitaxial Growth of GaAs on Si using a Graphene Buffer Layer', Adv. Functional Mat. **24** (42), 6629-6638 (2014).

9. Summary

We optimized a transfer process for CVD graphene onto GaAs substrate. We investigated effects of PMMA thickness, baking, copper etching time, different etchant batch, DI water bath time, SC2 cleaning and PMMA removal. The coverage and cleanness were optimized according to our best choice of these parameters. The graphene had large coverage areas, and few tears and wrinkles. The contaminations in graphene was reduced to a level that is compatible for epitaxial growth. To promote correlation between GaAs epilayer and substrate across graphene, sample annealing was used. It improved the surface roughness and conformity of graphene to substrate.

Our first few experiments of MOCVD growth produced undesirable nanowires in nucleation step. Contamination that caused these nanowire growth is the main obstacle to nucleation and therefore film growth. After investigating the effect of growth temperature, time, V/III flow ratio, precursor carrier gases and sample contaminations, we were able to obtain areas of good nucleation of the GaAs epilayer. Our attempts to grow a full epilayer showed that part of the growth are nonplanar films and part of them are rough planar film. We successfully exfoliated the epilayer from graphene/GaAs. We think both good and bad region of epilayer were exfoliated because most of the area covered by graphene came off. Although some graphene was peeled off together with the epilayer, some stayed on the GaAs substrate. This poor adhesion may be related to the polycrystallinity of the epilayer because adatoms could not interact with the substrate. In the exfoliated epilayer, Raman spectra show that two peaks around GaAs energy range, in contrast to only one peak in substrate. This may be caused by the roughness of the epilayer. EBSD measurement suggests that parts of the epilayer are polycrystalline while other parts show preferential alignment to the [111] direction. The polycrystalline areas have a more pitted surface while the aligned areas have a smooth surface. The preferential alignment to [111] was not observed by Y. Kim *et al*. and does not appear to be remote epitaxy. It may be caused by alignment between GaAs and the graphene layer. More investigation needs to be done to understand the aligned epilayer growth, to improve graphene adhesion to the substrate, and to further reduce the contaminations in transferred graphene and thus to improve the nucleation as well as the subsequent film growth of the epilayer. This process, if optimized, could be extended to other III-V semiconductors to reduce the substrate cost of related electrical and optical devices.

Acknowledgements

We would like to express our great appreciation to

- Our mentors Xiaoqing Xu for supervision, guidance, training, and SEM, and Karl Littau for feedback and advice
- Michelle Chen and Ning Wang for help with our graphene transfer process
- Andrey Malkovskiy for assistance with Raman spectroscopy
- Ricardo Peterson for Auger, Tzu-Ling Liu for AFM, Rui Yang for EBSD measurements
- Andrew Ceballos and Prof. Jonathan Fan
- SNF staffs for assistance with tools and trainings
- All of the E241 participants for helpful feedback during class
- Yunjo Kim and Prof. Jeehwan Kim for information about their growth process